Localization, mobility edges, and metal-insulator transition in a class of one-dimensional slowly varying deterministic potentials

S. Das Sarma, Song He, and X. C. Xie
Center for Theoretical Physics, Department of Physics, University of Maryland, College Park, Maryland 20742-4111
(Received 27 October 1989)

We study the localization properties of the one-dimensional nearest-neighbor tight-binding Schrödinger equation, $u_{n+1}+u_{n-1}+V_n u_n = E u_n$, where the on-site potential V_n is neither periodic (the "Bloch" case) nor random (the "Anderson" case), but is aperiodic or pseudorandom. In particular, we consider in detail a class of slowly varying potential with a typical example being $V_n = \lambda \cos(\pi \alpha n^{\nu})$ with $0 < \nu < 1$. We develop an asymptotic semiclassical technique to calculate exactly (in the large-n limit) the density of states and the Lyapunov exponent for this model. We also carry out numerical work involving direct diagonalization and recursive transfer-matrix calculations to study localization properties of the model. Our theoretical results are essentially in exact agreement with the numerical results. Our most important finding is that, for $\lambda < 2$, there is a metal-insulator transition in this one-dimensional model ($\nu < 1$) with the mobility edges located at energies $E_c = \pm|2-\lambda|$. Eigenstates at the band center ($|E| < |E_c|$) are all extended whereas the band-edge states ($|E| > |E_c|$) are all localized. Another interesting finding is that, in contrast to higher-dimensional random-disorder situations, the density of states, $D(E)$, in this model is not necessarily smooth through the mobility edge, but may diverge according to $D(E) \sim |E-E_c|^{-\delta}$. The Lyapunov exponent γ (or, the inverse localization length) behaves at E_c as $\gamma(E) \sim |E-E_c|^{\beta}$, with $\beta = 1-\delta$. We solve the exact critical behavior of the general model, deriving analytic expressions for $D(E)$, $\gamma(E)$, and the exponents δ and β. We find that λ, α, and ν are all irrelevant variables in the renormalization-group sense for the localization critical properties of the model. We also give detailed numerical results for a number of different forms of V_n.

I. INTRODUCTION

Study of localization induced by random disorder is now an old[1] and well established[2] subject. Comparatively new[3,4] is the subject of localization induced by a nonrandom, deterministic potential which is incommensurate with the underlying lattice. In both cases the one-dimensional nearest-neighbor tight-binding model describing the motion of a single electron in a one-dimensional lattice has been very helpful in elucidating physical details and in establishing rigorous results. The model is described by the equation

$$u_{n+1}+u_{n-1}+V_n u_n = E u_n \ , \tag{1}$$

where, for the sake of convenience, the strength of the nearest-neighbor hopping has been set equal to unity with no loss of generality. Equation (1) is the well-known[5] single-band one-dimensional tight-binding Schrödinger equation in a lattice within the nearest-neighbor approximation. In Eq. (1), u_n is the amplitude of the electronic wave function at the nth lattice site with V_n as the on-site diagonal potential and E the electronic eigenenergy. Choice of the diagonal potential V_n completely defines the model and the physical problem being studied. For example, periodic V_n is the usual Bloch case whereas Eq. (1) with a random V_n is the Anderson model. It is well-known that a V_n periodic in n has all its states extended whereas a wide class of random V_n produces[2,6] *all* localized states in one dimension. Intermediate between the periodic and the random situations is the incommensurate case[3,4] with a periodic V_n having a period incommensurate with the underlying lattice. The best-studied incommensurate potential is the incommensurate Harper's equation where V_n is modeled by an incommensurate trigonometric function. Aubry[3,4] showed that in such a potential either *all* electronic states are extended or *all* states are localized depending on the relative strengths of the potential and the hopping terms. When these two terms have "equal" strengths, all states are "critical" (neither localized nor extended), and the eigenenergies form a Cantor-set spectrum. Harper's equation and other incommensurate potentials have been extensively studied[7-10] in the recent literature.

In this paper we study a different class of one-dimensional potentials which are neither periodic nor random, and, which also do *not* belong to the simple incommensurate class mentioned above. These potentials are deterministic and aperiodic, and, are described by the equation

$$V_n \equiv \lambda \cos(\pi \alpha n^{\nu}) \ , \tag{2}$$

where α is a real number (which does *not* have to be an irrational in our case, however, we work with an irrational α so that for $\nu = 1$ we recover Harper's equation), and, λ is the strength of the potential having a magnitude in between 0 and 2. The positive exponent ν in Eq. (2) is taken to lie between 0 and 1 in this work so that Eq. (2) describes a very slowly varying potential in space. This

very slow spatial variation is crucial in producing the localization properties of the model being studied in this paper.

Our results (for $0<\nu<1$ and $0<|\lambda|<2$) are interesting because we find the existence of a mobility edge in this one-dimensional model. It is well-known that, in general, one-dimensional models do not allow for the existence of mobility edges. In particular, even for arbitrarily weak disorder (i.e., V_n random, but very small in magnitude) it has been rigorously[6] established that (at least, for hopping that is not too long ranged) the random Anderson model produces only (exponentially) localized electron eigenstates in one dimension for *all* energies (i.e., states both at the band center and band edges are localized). The incommensurate Harper's equation has no mobility edges either, with *all* states localized or extended depending on the strength of the incommensurate potential. To the best of our knowledge our discovery of the existence of mobility edges in this model is unique in the sense that it is the only known gapless spectrum of a one-dimensional Schrödinger operator allowing for the existence of a metal-insulator transition and mobility edges. We show that the model defined by Eqs. (1) and (2) with $0<\nu<1$ and $0<|\lambda|<2$ has extended states at the band center ($-E_c<E<E_c$) and localized states at the band edges $|E|>E_c$ with the mobility edges at $\pm E_c=\pm(2-|\lambda|)$. Note that the total bandwidth of the unperturbed tight-binding model ($\lambda=0$) defined by Eq. (1) is 4 with the absolute band edges at ± 2, whereas the perturbed system has absolute band edges at $\pm(2+|\lambda|)$.

The nature of localization and metal-insulator transition in this problem is substantially different from the usual Anderson-localization[2] problem (in three dimensions, since there are no mobility edges in lower dimensions for the random-disorder case) where the electronic density of states is known to be smooth through the mobility edge. In our problem we calculate the density of states exactly and show that it is singular at the mobility edges. In fact, the theorem asserting the smoothness of the density of states through $\pm E_c$ does not apply to our model because the potential defined by Eq. (2) has long-range coherence. This is discussed in more details in Secs. II and III.

We develop a theory (discussed in II) for the localization problem for a class of slowly varying aperiodic potentials of which Eq. (2) is just one example. Another specific example to be discussed in this paper is a piecewise constant square-well potential (with alternate heights $\pm\lambda$ at consecutive sites) of constant depth 2λ but of varying widths I_n at various sites defined by

$$L_n=q^n L_0 \ , \tag{3}$$

where q (>1) and L_0 are positive numbers. As n increases, this potential becomes more and more slowly varying in a fashion qualitatively similar to Eq. (2). On the basis of our exact asymptotic theory, we derive analytic expressions for the density of states and the Lyapunov exponent ("the inverse localization length") for the above two models [Eqs. (2) and (3)] and show that the theoretical results are essentially in exact quantitative agreement with our extensive numerical work to be presented in Sec. III.

Our numerical work (presented in III) involves direct diagonalization of the model Hamiltonian to directly calculate the eigenfunctions and the eigenenergies, from which the position of the mobility edges, the density of states, and the localization length are easily obtained. Since the direct diagonalization technique is computationally restricted only to systems of size 20 000 sites or less, we also directly calculate the Lyapunov exponent using the standard recursive transfer-matrix technique for systems as large as 10^8 sites. All our numerical results are in essentially exact agreement with the asymptotic theory. In the recent literature two other techniques have been employed to study the localization properties of this model. These are perturbation theoretic treatment developed[11,12] by Griniasty and Fishman and an analytic transfer-matrix calculation[13] due to Crisanti. Both of these techniques have their limitations. The perturbation theory (details are given in Appendix A), while giving correct results for $\nu\geq 2$, is invalid for $\nu<1$ and it does not predict the existence of a metal-insulator transition, inferring instead[12] that all states are extended in the model defined by Eq. (2) for $\nu<1$. The analytic transfer-matrix[13] calculation works *only* for the piecewise constant potential [Eq. (3)] and is, therefore, very limited in its scope. Its results for this model, however, agree exactly with our asymptotic theory. We should mention that our theory is also of limited validity because it is applicable only for very slowly varying potentials [i.e., only for $\nu<1$ in Eq. (2) or for $q>1$ in Eq. (3)].

We should point out that different aspects of the model defined by Eqs. (1)–(3) have been investigated[11–16] in the recent literature. Griniasty and Fishman[12] developed a perturbation theoretic approach concentrating mostly on $\nu\geq 2$. They showed that for $\nu\geq 2$ (*and*, for irrational α) V_n defined by Eq. (2) is pseudorandom and, then, Eq. (1) becomes equivalent to the random Anderson model producing only localized states in one dimension. The localization length for the $\nu\geq 2$ case was shown to be the same as that in the corresponding random case. Crisanti's transfer-matrix calculation[13] was motivated by an earlier short report[14] of ours in which we presented some of the essential results of this work. In a recent paper,[15] Thouless looked at the situation $1<\nu<2$ (with irrational α) and showed that all states (except exactly at the band center) are localized in that situation but the Lyapunov exponent vanishes very slowly as one approaches the band center. Thus, numerical work on the model for $1<\nu<2$ becomes unreliable as was earlier found in Ref. 12. In this paper we will mostly restrict ourselves to the regime $0<\nu<1$ except to make some qualitative remarks about the $\nu>1$ situation in discussions. Finally, in Ref. 16 very interesting mathematical and geometrical properties of the class of functions defined by Eq. (2) were studied in details without any reference to Eq. (1) or to localization properties of the tight-binding model.

The rest of the paper is organized in the following manner. In Sec. II we present our general theory, and, some heuristic arguments. In Sec. III we present our nu-

merical results comparing them with the theory. We provide a discussion with the conclusion in Sec. IV.

II. THEORY

We provide some preliminary heuristic arguments in II A, and, present our semiclassical asymptotic theory in II B. Since the cases with λ and $-\lambda$ are unitarily equivalent, we assume $\lambda > 0$ hereafter.

A. Preliminaries and heuristic arguments

The class of slowly varying potentials being studied here [Eqs. (2) and (3)] has the property that in the thermodynamic limit ($n \to \infty$), the potential difference between neighboring sites vanishing, or, the potential is locally constant. For example, from Eq. (1) we can write,

$$\frac{dV_n}{dn} = -\lambda\pi\alpha n^{\nu-1}\nu\sin(\pi\alpha n^{\nu}) , \tag{4}$$

implying

$$\left|\frac{dV_n}{dn}\right| \sim \frac{|\sin(\pi\alpha|n|^{\nu})|}{n^{1-\nu}} \to 0 \quad \text{as } n \to \infty$$

(remembering that $0 < \nu < 1$). Equivalently, $(V_{n+1} - V_n) \sim O(|n|^{\nu-1})$ which vanishes for large n, implying the local constancy of the potential. This asymptotic property of "local constancy" of V_n is crucial for the localization properties and the arguments presented here. The existence of a localization-delocalization transition in the model follows from the following asymptotic heuristic argument:

We write

$$u_n \sim z^n , \tag{5}$$

where z is a complex quantity. The Schrödinger equation [Eq. (1)] becomes

$$z^{n+1} + z^{n-1} - C_n z^n = 0 , \tag{6}$$

with

$$C_n = E - V_n . \tag{7}$$

The crucial point is that E is a global property and V_n is locally almost a constant; therefore, the function C_n is a local constant for large n:

$$C_n \approx C \text{ locally independent of } n \text{ for large } n . \tag{8}$$

Equation (6) then becomes

$$z^2 - Cz + 1 = 0 , \tag{9}$$

with the complex solutions

$$z_{1,2} = \tfrac{1}{2}(c \pm \sqrt{c^4 - 4}) . \tag{10}$$

From Eq. (10) we conclude that the amplitude is complex and $|z_1| = |z_2| = 1$ or extended if $|C| < 2$ whereas it is real or localized if $|C| > 2$. Taking into account the fact that $C \approx C_n = E - V_n = E - \lambda\cos(\pi\alpha n^{\nu})$ we conclude that the conditions for the extended or localized solutions are the following:

$$|C|_{\max} < 2 \Longrightarrow |E| < 2 - \lambda \quad \text{(extended)} , \tag{11a}$$

$$|C|_{\max} > 2 \Longrightarrow |E| > 2 - \lambda \quad \text{(localized)} , \tag{11b}$$

where $|C|_{\max} = |E| + \lambda$ is the maximum possible value of $|C|$.

Equation (11) implies that there is a metal-insulator transition in the system at the mobility edges $E_c = \pm|2 - \lambda|$ as the energy is increased in magnitude from the band center ($E = 0$) to the band edges ($E = \pm|2 + \lambda|$). Note that the heuristic argument leading to Eq. (11), which establishes the mobility edges in the model, is based entirely on the local constancy of the model potential in the large-n limit. We emphasize that the wave function in the model is a local property, whereas the energy is a global property of the model. What we have established above is that the wave function decays locally for $|E| > E_c$, whereas it is locally extended for $|E| < E_c$. These locally localized states are actually globally localized because there is no energy degeneracy in the problem since the slowly varying potential never repeats itself, and, therefore, no resonance is possible. The locally extended solutions remain globally extended because the condition for an extended solution in Eq. (11) is satisfied at every lattice site so the state is "locally" extended at every site.

We can better quantify the above conclusion by considering the wave-function overlap and energy degeneracy between two neighboring wells in the large-n limit. It is easy to solve the harmonic oscillator eigenvalue problem around the potential minimum in the $N(\to \infty)$-site problem. One finds that the wave-function overlap between neighboring sites goes down exponentially as $e^{-aN(\nu-1)}$, whereas the energy difference between neighboring minima decreases algebraically as $N^{\nu-1}$. This ensures that no resonance is possible in the large-N limit, guaranteeing that the heuristic argument given above is actually exact in the thermodynamic limit, and, the "local" mobility edges defined by Eq. (11) are rigorously global.

Before developing the exact asymptotic theory in II B, we introduce some notations. There are two related quantities of particular interest in the localization problem. These are the electronic density of states $D(E)$ and the Lyapunov exponent. The definition of $D(E)$ is the usual one,

$$D(E) = \sum_j \delta(E - E_j) , \tag{12}$$

where E_j is eigenenergy spectrum. The Lyapunov exponent $\gamma(E)$ is the inverse localization length which gives the asymptotic behavior of the energy wave function according to

$$|\psi_j(x)| \sim e^{-\gamma_j x} , \tag{13}$$

where $\gamma_j \equiv \gamma(E_j)$. If ξ_0 is the localization length defined by the asymptotic relation $\psi(x) \sim e^{-x/\xi_0}$, then the Lyapunov exponent is seen to be the inverse localization length:

$$\gamma \equiv \xi_0^{-1} . \tag{14}$$

The following equations[17] relate the Lyapunov exponent to the eigenenergies and the eigenfunctions of the model:

$$\gamma(E_j)=\frac{1}{N-1}\sum_{j\neq l}\ln|E_j-E_l| , \tag{15a}$$

$$=\frac{1}{N}\sum_{n=1}^{N}\ln\left|\frac{u_{n+1}}{u_n}\right| , \tag{15b}$$

where N is the number of sites in the system. Equations (15a) and (15b) are useful in numerically obtaining γ by using the direct diagonalizational and the transfer-matrix techniques, respectively, as we will discuss in III.

The density of states and the Lyapunov exponent are related by the following equation:[17]

$$\gamma(E)=\int dE'\,D(E')\ln|E'-E| . \tag{16}$$

For extended states below the mobility edge ($|E|<E_c$), $\gamma(E)=0$. Of particular interest is the behavior of the Lyapunov exponent at the mobility edge:

$$\gamma(E)\sim|E-E_c|^{\beta} , \tag{17}$$

around $E\gtrsim E_c$. Similarly, the behavior of the density of states at the mobility edge can be written as

$$D(E)\sim|E-E_c|^{-\delta} . \tag{18}$$

The critical exponents β and δ are clearly related [cf. Eq. (16)] by the equation

$$\beta=1-\delta \text{ with } \delta>0 . \tag{19}$$

In Sec. II B we develop a semiclassical asymptotic theory based on the slowly varying nature of V_n. The theory is exact in the thermodynamic limit and enables us to obtain analytic formulas for $D(E)$, $\gamma(E)$, and the critical exponents β and δ for an arbitrary potential belonging to the slowly varying one-dimensional class we are studying in this paper.

B. Semiclassical asymptotic theory

Mathematically the class of model potentials being studied here can be defined as

$$V_n=f(n^{\nu}) , \tag{20}$$

with $\nu<1$. In Eq. (20), $f(x)$ is a periodic function with period T and its values are within $\pm\lambda$. The conditions $\nu<1$ makes the diagonal potential V_n slowly varying which, as has been argued in Sec. II A, can be regarded locally as a constant. Using the local constancy of V_n we have shown (in Sec. II A) that $|E|>E_c$ remain globally localized because the incommensurate nature of V_n ensures that no energy degeneracy exists in the model. Similarly, the locally extended eigenstates remain globally extended because the condition for local extension is satisfied at every local site.

We now extend the arguments of Sec. II A based on the local constancy of V_n to calculate the density of states (and, equivalently, the Lyapunov exponent) of the model. We use the semiclassical WKB technique[18] which is ideally suited for this problem due to the slowly varying nature of the potential. We emphasize two aspects of our theory. (i) In the thermodynamic limit of very large N (where N is the total number of lattice sites in the system), our semiclassical theory is asymptotically *exact* because the potential V_n is asymptotically exactly constant; (ii) in the usual (i.e., random potential) localization problem, WKB technique is *not* a useful theoretical tool because it is essentially a local theory, however, in our problem the wave-function overlap between neighboring wells vanishes (faster than energy degeneracy) in the larger-N limit making the semiclassical theory asymptotically exact (this claim is further corroborated by the very good agreement between our theory and the numerical results presented in Sec. III and also by the exact agreement between our analytic formulas and the transfer-matrix results[13] of Crisanti for the square-well model).

The first step in our theory is to make a continuum approximation for the basic tight-binding equation [i.e., Eq. (1)] of the model. For this purpose, we consider the block of lattice in the period after the site $N\gg1$. Under the substitution

$$n=N+l , \tag{21}$$

Eq. (1) becomes

$$U_{N+l+1}+U_{N+l-1}=(E-V_{N+l})U_{N+l} . \tag{22}$$

Restricting ourselves to the specific potential $V_n=\lambda\cos(\pi\alpha n^{\nu})$, Eq. (22) becomes

$$U_{N+l+1}+U_{N+l-1}=[E-\lambda\cos(\pi\alpha N^{\nu}+\pi\alpha\nu N^{\nu-1}l)]U_{N+l} . \tag{23}$$

Redefining $U_{N+l}=U(x)$ with $x=l/N^{1-\nu}$, Eq. (23) gives

$$U(x+N^{\nu-1})+U(x-N^{\nu-1})=[E-\lambda\cos(\pi\alpha\nu x+\phi_0)]U(x) . \tag{24}$$

Since we are working in a full period of the periodic potential $\lambda\cos(\pi\alpha\nu x+\phi_0)$, we may discard ϕ_0; then

$$U(x+N^{\nu-1})+U(x-N^{\nu-1})=[E-\lambda\cos(\pi\alpha\nu x)]U(x) . \tag{25}$$

We introduce

$$U(x)=A(x)e^{\phi(x)/N^{\nu-1}} \tag{26}$$

with $A(x)$ a slowly varying function of x. Then, to the lowest order in $N^{\nu-1}$ Eq. (25) reduces to

$$\frac{d\phi}{dx}=\cosh^{-1}\left[\frac{E-\lambda\cos(\pi\alpha\nu x)}{2}\right] . \tag{27a}$$

Thus the site-average change in $\phi(x)$ through one period is

$$\phi/L=\frac{1}{L}\int_0^{2/\alpha\nu}dx\,\cosh^{-1}\left[\frac{E-\lambda\cos(\pi\alpha\nu X)}{2}\right] \tag{27b}$$

with $L=(2/\alpha\nu)N^{1-\nu}$ being the number of lattice sites in

that period. Now, if we define $\Gamma_N(E)=\phi/(LN^{\nu-1})$, then

$$\Gamma_N(E)=\frac{1}{2\pi}\int_0^{2\pi}d\theta\cosh^{-1}\left[\frac{E-\lambda\cos\theta}{2}\right]. \tag{28}$$

From the convergence of the limit $\lim_{N\to+\infty}\phi/LN^{\nu-1}$, we see that the function $\Gamma(E)=\lim_{N\to+\infty}\Gamma_N(E)$ exists. Furthermore, the Lyapunov exponent $\gamma(E)$ and the density of states $D(E)$ can be found from the equations

$$\gamma(E)=\mathrm{Re}\Gamma(E)\ , \tag{29}$$

$$D(E)=-\frac{1}{\pi}\frac{d}{dE}\mathrm{Im}\Gamma(E)\ . \tag{29'}$$

Obviously, the above derivation can be generalized to any quasiperiodic potential described by the function $f(x)$, giving, in general,

$$D(E)=\frac{1}{T}\int_{-T/2}^{T/2}dx\cosh^{-1}\left[\frac{E-f(x)}{2}\right]. \tag{28'}$$

Combining (28') and (29'), we get

$$D(E)=\begin{cases}0, & \text{with } |E-f(x)|>2 \text{ (for all } x)\ , \\ \dfrac{1}{2\pi}\dfrac{1}{T}\displaystyle\int_{-T/2}^{T/2}dx\ \mathrm{Re}\left[\dfrac{1}{\left[1-\left[\dfrac{E-f(x)}{2}\right]^2\right]^{1/2}}\right] & \end{cases} \tag{30}$$

$$\text{otherwise}\ . \tag{31}$$

Remembering that the extrema of $f(x)$ are at $\pm\lambda$ as x goes through a whole period, Eq. (31) indicates that the absolute band edges for the model are now located at $\pm(2+\lambda)$ because there is no density of states outside this energy region. Inside the band, i.e., for $|E|<2+\lambda$. Equation (30) gives us the density of states for a general slowly varying potential satisfying Eq. (20).

The two cases studied numerically in this paper are the cosine potential [Eq. (2)] and the square-well potential [Eq. (3)]. For both of these models the exponents β and δ can be exactly calculated by substituting the appropriate functions for $f(x)$ in Eqs. (28) and (30). We get

$$\beta=1,\quad \delta=0 \quad \text{for the cosine model}\ , \tag{32}$$

and

$$\beta=\tfrac{1}{2},\quad \delta=\tfrac{1}{2} \quad \text{for the square-well model}\ . \tag{33}$$

Note that both of these satisfy the scaling relation $\beta=1-\delta$ [Eq. (19)] as they should for an analytic $f(x)$. Equations (32) and (33) imply that the density of states for both the models are divergent at the mobility edge according to

$$D(E\sim E_c)\sim\begin{cases}\ln|E-E_c| & \text{(the cosine mode)}\ , \quad (34a)\\ |E-E_c|^{-1/2} & \text{(the square-well mode)}\ . \quad (34b)\end{cases}$$

Our numerical work to be presented in Sec. III verifies all these theoretical predictions rather spectacularly.

Before concluding this section, we discuss the surprising singularity in our calculated density of states for these slowly varying potentials. At first sight this result seems to be in error because in three-dimensional Anderson-localization problem $D(E)$ is smooth through the mobility edge and, indeed, there is a theorem[19] asserting that it should be so. The singularity in our $D(E)$ at $E=E_c$ is, of course, not an error (it shows up clearly in our numerical work) and is a peculiar feature of the slowly varying nature of our localizing potential. Edward and Thouless showed[19] that $D(E)$ should be regular in the region defined by

$$|E+\lambda|>z \quad \text{and} \quad |E-\lambda|>z\ , \tag{35}$$

where z is the lattice coordination number. In the (three-dimensional) Anderson model the mobility edge E_c lies inside the regular region defined by Eq. (35) and, therefore, the density of states is smooth through E_c in the random Anderson model. In our one-dimensional problem (we note that there is *no* mobility edge in the one-dimensional Anderson model, *all* states being localized), however, $z=2$, and, consequently $\pm E_c=\pm(2-\lambda)$ are coincident with the boundaries of the region defined by Eq. (35). Thus, the theorem asserting the smoothness of $D(E)$ does not apply to our model and there exists no theoretical argument to indicate that the density of states must be regular at the mobility edge. As we have shown theoretically in this section (and, numerically in Sec. III), the density of states of the class of one-dimensional potentials being studied in this paper is allowed to be divergent at E_c and the exact nature of the divergence depends on the particular form of the on-site potential V_n. In fact, for the square-well potential we can calculate $D(E)$ algebraically for all values of E by substituting

$$f(x)=\begin{cases}\lambda & \text{for } 0\le x\le T/2\ , \\ -\lambda & \text{for } -T/2<x<0\ ,\end{cases} \tag{36}$$

in Eq. (30) and then carrying out the resulting integrations analytically. We get, after normalizing the density of states,

$$D(E)=\begin{cases}\dfrac{1}{4\pi}\left\{\left[1-\left[\dfrac{E-\lambda}{2}\right]^2\right]^{-1/2}+\left[1-\left[\dfrac{E-\lambda}{2}\right]^2\right]^{-1/2}\right\} & \text{for } |E|<E_c \\ \dfrac{1}{4\pi}\left\{\left[1-\left[\dfrac{|E|-\lambda}{2}\right]^2\right]^{-1/2}\right\} & \text{for } E_c<|E|<E_B\equiv 2+\lambda\end{cases} \tag{37}$$

where $\pm E_B = \pm(2+\lambda)$ are the absolute band edges and $\pm E_c = \pm(2-\lambda)$ are the mobility edges. Equation (37) exactly agrees with the transfer-matrix result[13] of Crisanti and with our numerical results which we present next. We emphasize that the divergent behavior of $D(E_c)$ is *not* a generic feature of the class of slowly varying potentials being studied in this paper (see Appendix B)—it is only that for certain specific forms of V_n, $D(E)$ could be divergent. There are potentials (e.g., a curved sawtooth potential) for which $D(E)$ is continuous through E_c.

III. NUMERICAL RESULTS

Our asymptotic semiclassical theory presented in II is exact in the thermodynamic limit. In this section we present detailed numerical results in support of the theoretical claims derived in II. We have employed two alternative numerical schemes for our computation: (i) We have directly diagonalized the model Hamiltonian defined by the tight binding equation (1) to obtain the eigenfunctions u and the eigenenergies E. Within the nearest-neighbor approximation, the tight-binding Hamiltonian is a tridiagonal matrix enabling us to diagonalize fairly large systems up to 50 000 sites in size (even though most of our simulations are on smaller systems typically 1000–10 000 sites in size). Once the eigenfunctions and the eigenenergies are calculated, it is fairly straightforward to calculate the Lyapunov exponent $\gamma(E)$ [cf. Eq. (15a)] and the density of states $D(E)$ [cf. Eq. (12)] by directly using their definitions. (ii) We also obtain the Lyapunov exponent directly for very large (up to 10^8 lattice sites in size) systems by using the transfer-matrix technique on the nearest-neighbor Hamiltonian. This is done in the usual manner[17] by using Eq. (15b) and the transfer-matrix technique. Our calculated $\gamma(E)$ using the transfer-matrix technique agrees completely with our direct diagonalization results.

All our numerical results are in excellent agreement with the theory developed in II, showing that the asymptotic theory works very well even for finite systems where $V(x)$ is clearly not a constant locally. This is not obvious at the outset because the theory asserts that many of the quantities of interest (e.g., E_c, β, δ) are independent of the explicit values of the parameters (e.g., α, ν) defining the model. Even the parameter λ enters only in determining the mobility edge $E_c = |2-\lambda|$, but *not* the critical exponents β and δ. In fact, some manipulations (see Appendix B for details) of Eq. (28) show that the critical exponent β for the localization length ($\gamma^{-1} \sim |E - E_c|^{-\beta}$) can be written as

$$\beta = \frac{1}{2} + \frac{1}{\sigma} , \tag{38}$$

where σ is the local curvature of the potential near its extrema in the large n limit, i.e., $|V_n|$ behaves in the following manner near its minimum and *maximum* in the large-n limit:

$$|V_n| \sim |\Delta n|^{\sigma} , \tag{39}$$

with $n = n_0 + \Delta n$ and V_{n0} is an extremum. For the cosine and the square-well models, σ is given by

$$\sigma = \begin{cases} 2 \text{ for the cosine model} , & \text{(40a)} \\ +\infty \text{ for the square-well model} , & \text{(40b)} \end{cases}$$

which produces

$\beta = 1$ for the cosine model

and

$\beta = \frac{1}{2}$ for the square-well model ,

as we have already stated. It follows ($\delta = 1 - \beta$) that $D(E)$ has a logarithmic and inverse square-root singularities for the above models, respectively. More details on the singularities of $D(E)$ are given in Appendix B.

Thus, according to the asymptotic theory, E_c is determined only by λ (and, *not* influenced by any other parameters of the model) whereas β and δ are universal numbers determined only by the algebraic forms of the potential functions and *not* by the explicit parameters determining the details of the potential. Our detailed numerical results presented in this section fully verify this somewhat surprising result. Thus, the variables λ, α, and ν are all irrelevant from a renormalization group viewpoint for the critical properties of the model.

Our numerical results are presented in Figs. 1–8. Where appropriate, we have compared our direct numerical results with the analytic formulas derived in the last section. We present results for the two model potentials introduced in I, namely, the cosine model [Eq. (2)] and the square-well model [Eq. (3)]. In each case we show typical localized and extended wave functions (obtained by the direct diagonalization), the Lyapunov exponent $\gamma(E)$, and the density of states $D(E)$ as well as the "localization correlation length" ξ defined through the integral

$$\int_{-\xi/2}^{\xi/2} dx \, |u(x - x_0)|^2 = P , \tag{41}$$

where x_0 is the center ("the peak") of a particular wave function u and P is a preassigned number chosen close to unity (we choose $P = 0.99$, however, we have varied P systematically between 0.95 and 0.99 to check our results). For extended states normalization ensures that ξ would be of the order of the system size, whereas for localized states ξ would be small (of the order of γ^{-1}, much smaller than the system size). Thus, the metal-insulator transition would manifest itself by a large drop in the value of ξ from below $|E_c|$ to above $|E_c|$ as the energy is changed. For $E < |E_c|$, ξ would be a constant equal to the system size whereas ξ is much smaller than the system size below $|E_c|$. This behavior is seen in our results.

In Figs. 1 and 2 we show our results for the piecewise-constant square-well potential [Eq. (3)], where the potential alternately varies between $\pm\lambda$ with a variable width defined by Eq. (3). For the numerical results shown here we have chosen $L_0 = 10$, $q = 1.1$, and $\lambda = 0.4$ in Eq. (3). Our results are qualitatively very similar for other values of these parameters. In Fig. 1 we show typical localized ($|E| > E_c = 1.6$) and extended ($|E| < E_c = 1.6$) eigenstates for this potential for four different energies. Note that the localized wave functions develop more and more "wiggles" in it as one moves away from the absolute band

edges. In Fig. 2 we show our calculated density of states $D(E)$ and the Lyapunov exponent $\gamma(E)$ for the square-well model. In Fig. 2(a) the $D(E)$ can be seen to have an inverse square-root singularity at $E=E_c$. We have used a best-fit analysis to obtain the exponent δ from our numerical results and we find $\delta=0.5$ to a high degree of accuracy. This is in agreement with our theoretical prediction. In fact, our theoretical $D(E)$ given in Eq. (37) agrees extremely well with our numerical $D(E)$. In Figs. 2(b) and 2(c) we show our numerical results for the Lyapunov exponent $\gamma(E)$ which clearly shows the existence of mobility edges at $E=\pm E_c=\pm|2-\lambda|$. The numerical γ agrees very well with our theoretical prediction given in Sec. II. Our best-fit analysis gives the critical exponent $\beta=0.5$ in exact agreement with the theory.

We have obtained numerical results for the square-well model using other values of the parameters λ, L_0, and q. In agreement with our theory we find that, except for a dependence of the mobility edge on the parameter λ according to the theoretical prediction $E_c=|2-\lambda|$, there is no dependence of E_c, β, and δ on the parameters of the model.

In Figs. (3)–(11) we show our numerical results for the cosine model defined by Eq. (2). In Fig. 3 we show typical localized and extended eigenstates for four different energies using parameters $\lambda=0.4$, $\pi\alpha=0.2$, and $\nu=0.7$. States with $|E|>E_c=1.6=2-\lambda$ are all found to be localized whereas states below E_c are extended in agreement with the theory. Again, the localized states have more wiggles in them as one moves toward the mobility edge from the absolute band edge.

In Fig. 4 we show calculated $D(E)$ [Figs. 4(a) and 4(b)], $\gamma(E)$ [Fig. 4(c)], and $\xi(E)$ [Fig. 4(d)] for the cosine model using the same parameters in Fig. 3. The *average* density of states shown in Fig. 4(b) is obtained by taking an average over the irrelevant variable α (in the internal $0.2\le\pi\alpha\le0.8$). We have explicitly verified that the divergence in $D(E)$ at $E=E_c$ is indeed logarithmic as demanded by the theory. Similarly, the Lyapunov exponent in Fig. 4(c) can be seen to vanish at $E=E_c$ in a

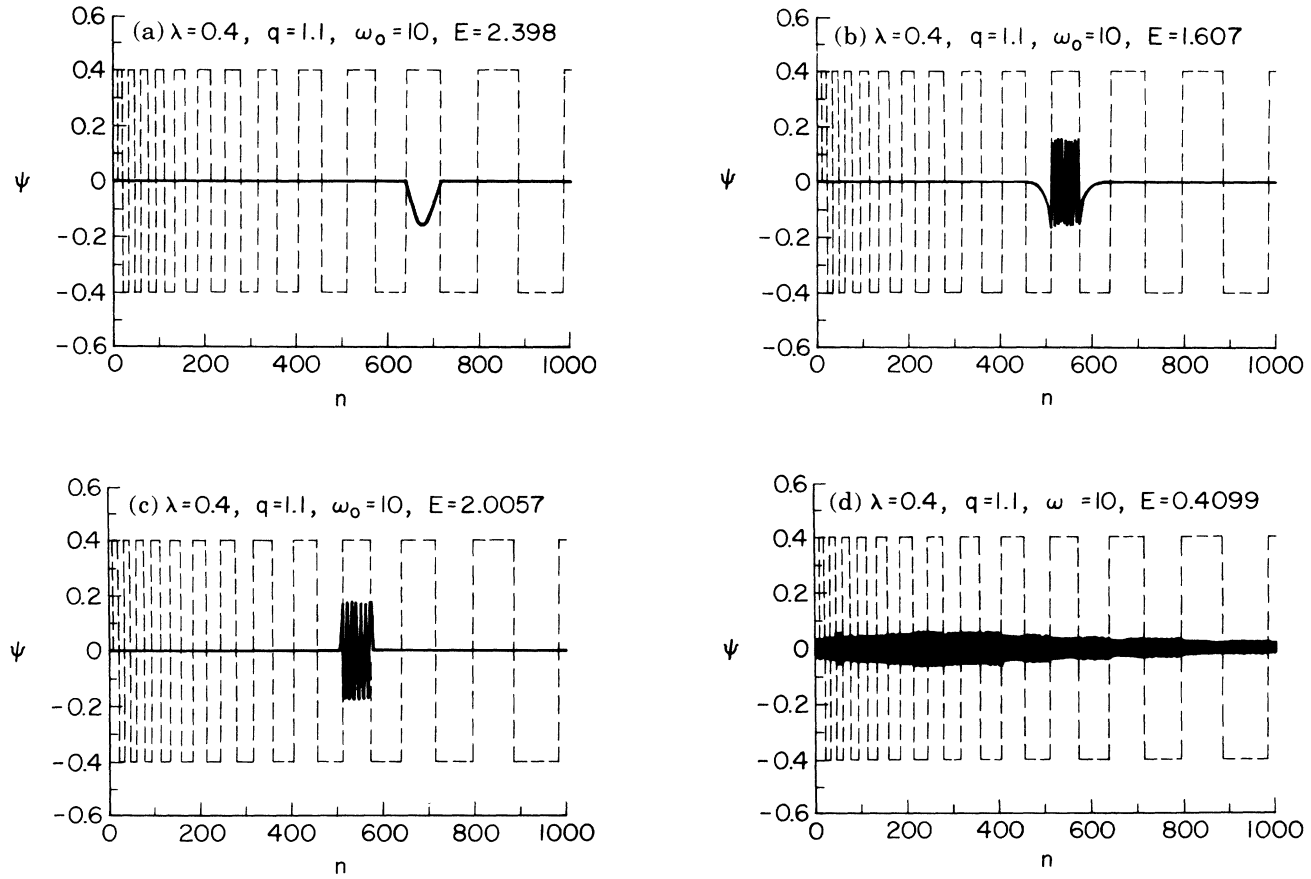

FIG. 1. (a) An eigenstate near the upper band edge for the square-well potential. The potential itself is also plotted in the background. The square-well potential is defined as follows. The well widths are $L_n=L_0q^n$ and the well heights are λ or $-\lambda$ alternatively along the lattice, where $L_0=10$, $q=1.1$, and $\lambda=0.4$ in this case. (b) An eigenstate just above the mobility edge $E_c=1.6$ for the potential defined in (a). (c) A typical localized eigenstate for the square-well potential. (d) A typical eigenstate for the square-well potential.

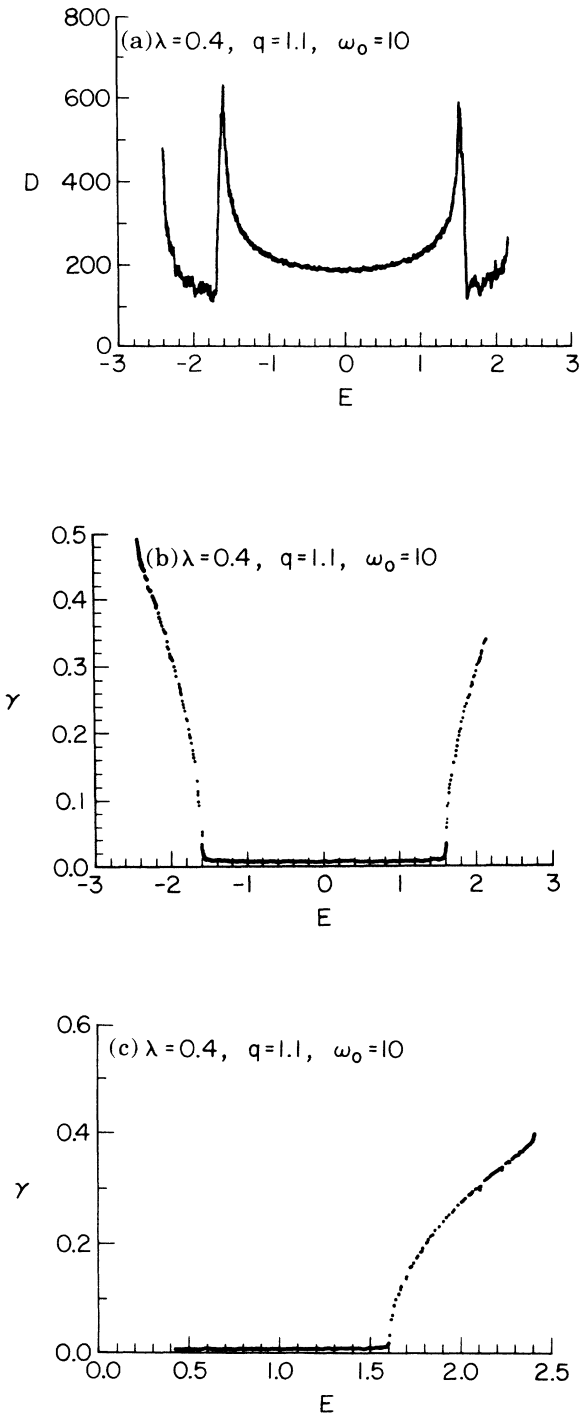

FIG. 2. (a) The density of states, $D(E)$, for the square-well potential defined in Fig. 1. One can see clearly that the DOS is singular at the mobility edges which are at $E_c=1.6$ or $E_c=-1.6$ in this case. This singularity is identified to be a power law with an exponent $\delta=0.50$ by our numerical calculation, where δ is defined by $D\sim|E-E_c|^{-\delta}$. (b) The Lyapunov exponent vs energy for the square-well potential defined in Fig. 1. One can see that the mobility edges are at $E_c=1.6$ or $E_c=-1.6$. (c) The singular behavior of the Lyapunov exponent γ near the upper mobility edge for the square model. This singularity is identified to be a power law with an exponent $\beta=0.50$ where β is defined by $\gamma\sim(E-E_c)^{\beta}$.

linear fashion, making the critical exponent β to be unity in agreement with the theory. Finally, the behavior of numerically calculated $\xi(E)$, the localization correlation length defined by Eq. (41), can be seen in Fig. 4(d) to clearly show the existence of a mobility edge at $E=E_c=2-\lambda$.

In Fig. 5 we show some of our typical transfer-matrix calculations of the Lyapunov exponent for energies very close to the mobility edge. The asymptotic behavior of $\gamma(E)$ for very large systems shows the existence of a mobility edge at $E=E_c=|2-\lambda|$ with states above E_c being localized so that $\gamma(|E|>E_c)$ converges to a nonzero constant whereas the states below E_c are extended with $\gamma(|E|<E_c)$ converging towards a limiting value of zero in the thermodynamic limit. Note that the closer one is in energy to the mobility edge, the longer the system must be for the convergent asymptotic behavior to show up. We have checked these explicit values of $\gamma(E)$ against our theoretical estimates based on Eqs. (28), obtaining very good agreement between the theory and the numerical results.

We have varied λ, α, and ν in our numerical work on the cosine model to ensure that α and ν are indeed "irrelevant" variables, whereas λ is relevant only in determining the mobility edge E_c. In agreement with the theory we find that the exponents β and δ do not depend on the actual values of the parameters λ, α, and ν. In Fig. 6 we show our calculated density of states [Figs. 6(a) and 6(b)] and the Lyapunov exponent [Fig. 6(c)] for a value of $\nu=0.9$ different from that ($\nu=0.7$) used in Fig. 4. The other parameters have been kept the same. As one can see E_c, β, and δ do not depend on the irrelevant variable ν. The same is true of the irrelevant parameter α.

In Fig. 7 we show our calculated $D(E)$ and $\gamma(E)$ for the cosine model by changing the value of the parameter λ to $\lambda=2.0$, keeping the other parameters the same ($\nu=0.7$, $\pi\alpha=0.2$) as that in Figs. 3–5. The two mobility edges at $\pm E_c$ now merge and shift to the center of the band at $E_c=2-\lambda=0$. Thus the inset of Fig. 7(a) of the averaged $D(E)$ is logarithmically singular at $E=E_c=0$, whereas in Fig. 7(b) $\gamma(E)$ is finite everywhere except at $E=E_c=0$, where it vanishes linearly, as it should for the cosine model.

In Fig. 8 we show the ratio of the total number of extended to localized states in the cosine model ($\nu=0.7$, $\pi\alpha=0.2$; $N=16\,400$) as a function of the potential strength λ on a log-log plot. Our semiclassical theory given in the last section can be used to derive the asymptotic divergent behavior of this ratio as λ is reduced. For the cosine model we find

$$R(\lambda\rightarrow 0)\sim\lambda^{-1/2}\,, \tag{42}$$

where

$$R=\frac{\text{No. of extended states}}{\text{No. of localized states}}\,. \tag{43}$$

From our numerical fit to the result shown in Fig. 8 we find the critical exponent for the divergence of R to be 0.5, in good agreement with Eq. (42).

In Fig. 9 we show a direct comparison between our analytic theory and the numerical results for the cosine model. In Figs. 9(a) and 9(b), respectively, we show our direct numerical results for the density of states $D(E)$ and the Lyapunov exponent $\gamma(E)$ taking $\lambda=1.2$ and $\nu=0.7$, whereas the corresponding analytic results are shown as insets in the same figures. This agreement between the asymptotic analytic theory and the direct numerical simulation for $\gamma(E)$ and $D(E)$, which is essentially exact, is found for *all* the results shown in this paper.

Finally, we conclude this section by showing some results for a third and more general type of slowly varying potential, namely, a curved sawtooth potential defined by

$$V_n(x)=\lambda\left[1-\left|\frac{2x}{T_n}-1\right|^{\sigma}\right]$$

with $V_n(x)$ giving the potential in the nth period and the period T_n is given by

$$T_n=T_0 q^n .$$

Here the extreme of V is given by $V(x)\sim V_0\pm V_1 x^{\sigma}$. This curved saw-tooth potential is different from the other two (viz., the cosine and the square-well) specific potentials studied in this paper in the sense that its density of states $D(E)$ is not divergent through $E=E_c$, provided $\sigma<2$. We note that for the cosine and the square-well models [cf. Eq. (40)] the values of σ and ∞, respectively. As we show in Appendix B, $D(E)$ diverges only for $\sigma\geq 2$. We also point out that the curved saw-tooth (CST) potential is equivalent to the cosine and the square-well potentials, respectively, for $\sigma=2$ and ∞.

In Figs. 10(a)–10(d) and 11(a)–11(d) we show, respectively, the calculated density of states and the Lyapunov exponent for the CST model for a number of different values of the parameter σ ($=0.75$, 1.0, 1.5, and 4.0) with $\lambda=0.4$. Note that the location of the mobility edge is determined solely by λ: $E_c=\pm|2-\lambda|=\pm 1.6$. For $\sigma<2$ [i.e., Figs. 11(a)–11(c)] the density of states is nondivergent at $\pm E_c$ whereas for Fig. 11(d), σ being 4, $D(E)$ is

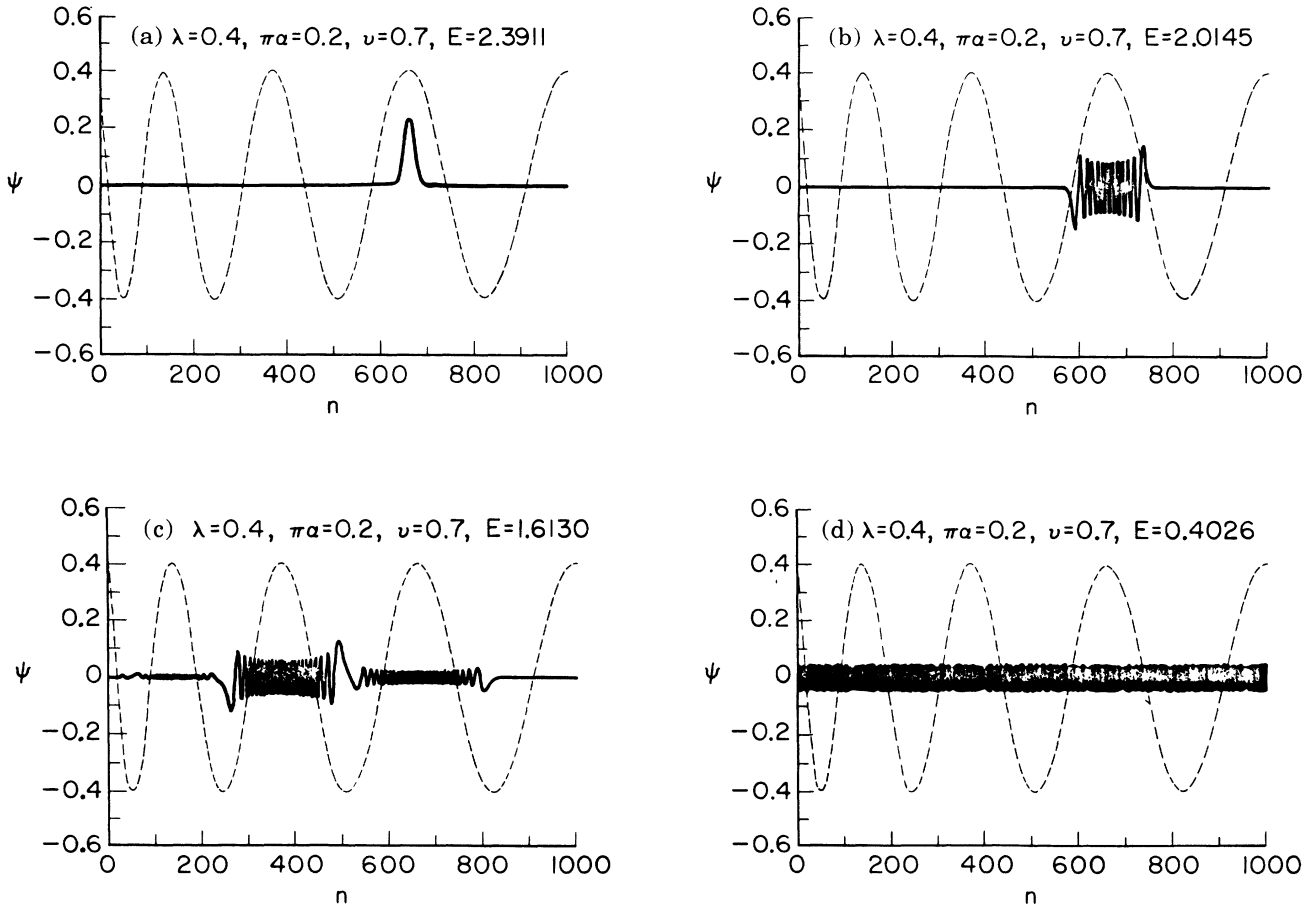

FIG. 3. (a) An eigenstate near the upper band edge for the cosine potential defined by $V_n=\lambda\cos(\pi\alpha n^{\nu})$ with $\nu=0.70, \pi\alpha=0.20$, and $\lambda=0.40$. The potential is shown in the background. (b) A typical localized eigenstate for the cosine potential. (c) An eigenstate just above the upper mobility edge $E_c=1.6$. (d) A typical extended eigenstate for the cosine potential.

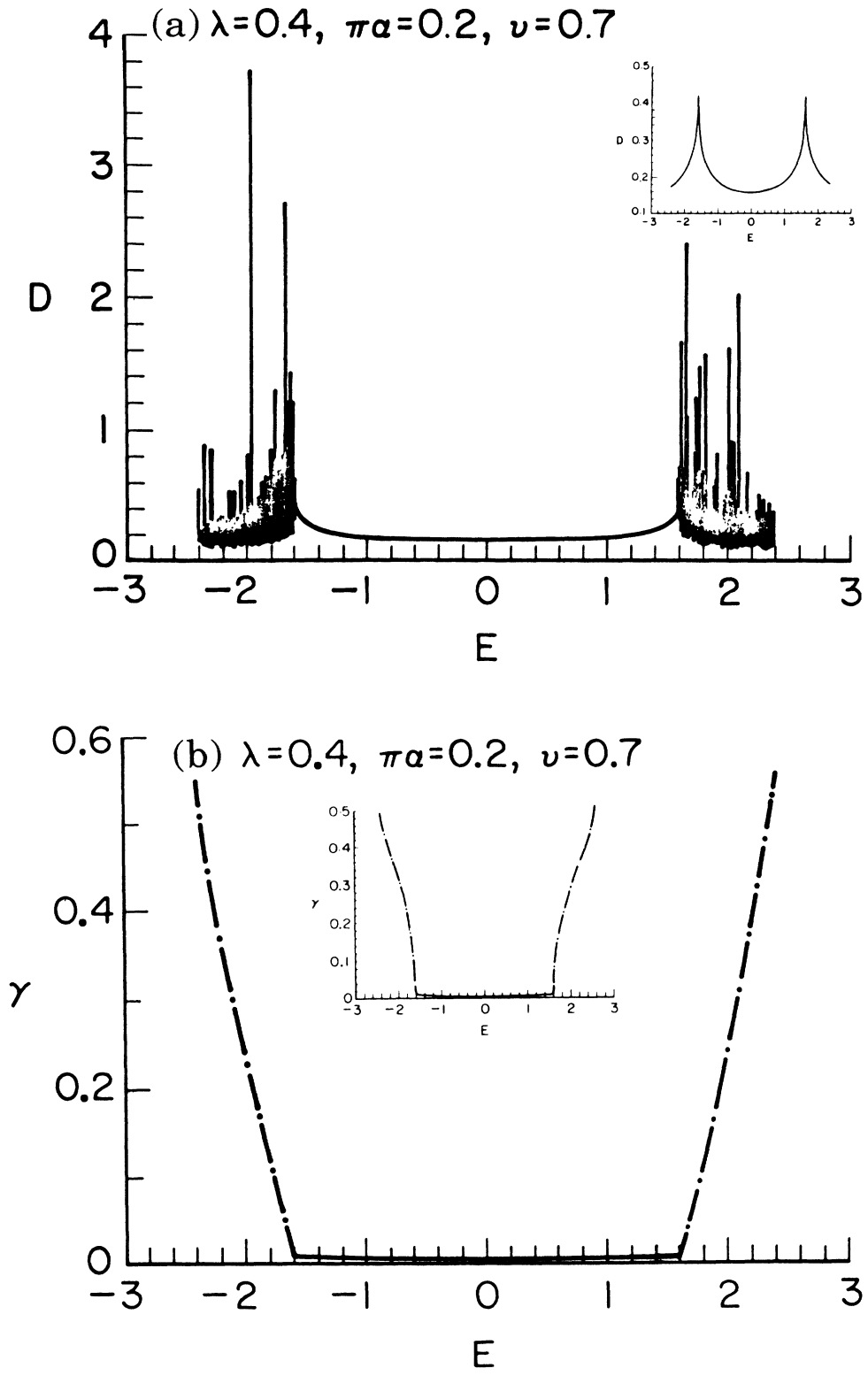

FIG. 4. (a) The density of states (DOS) for the cosine potential defined in Fig. 3. One can see a dramatic change when the energy passes through the mobility edges. The inset shows the average DOS for the cosine potential. The average is taken over the irrelevant variable α which is usually taken to be in the interval [0.2,0.8]. As can be identified by our numerical calculation or calculated by the WKB theory, this divergence in the DOS is logarithmic. (b) The Lyapunov exponent γ vs energy for the cosine potential. One can see that the mobility edges are at $E_c = 1.6$ or $E_c = -1.6$. The singular behavior of γ is identified to be linear by our numerical calculation or by the WKB theory. The inset is for the square-well potential. (c) The localization length ξ vs energy near the upper mobility edge. The saturation below $E_c = 1.60$ is due to the finite-size effect. [$\xi(p)$ is defined in the text.]

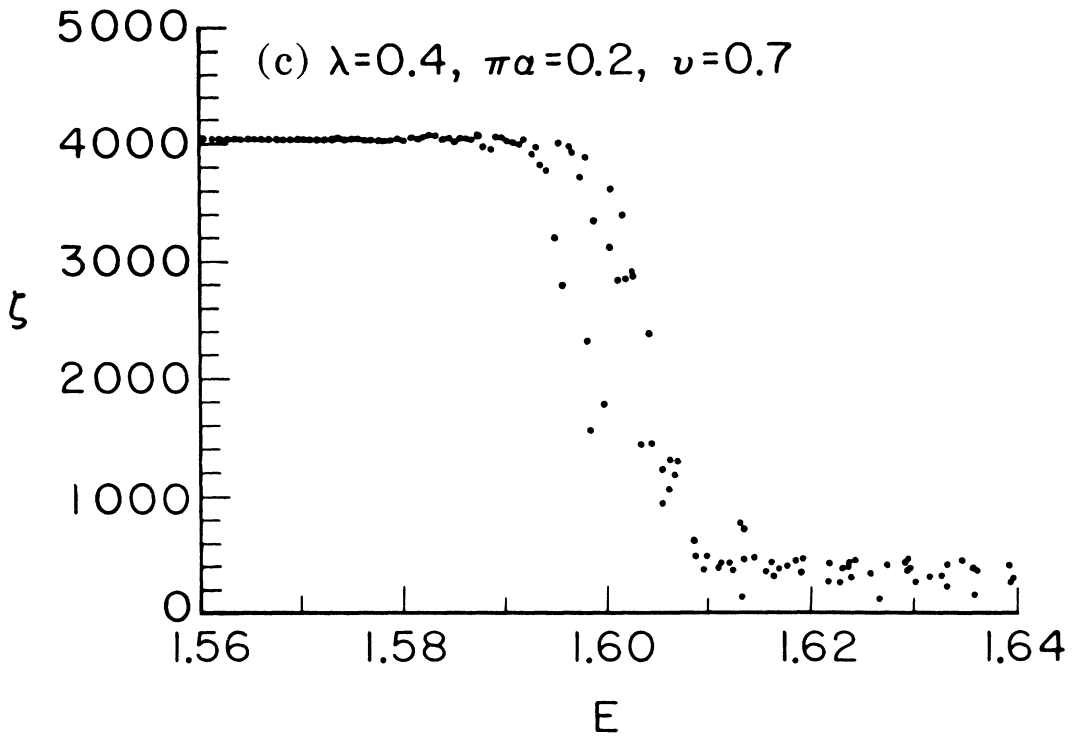

FIG. 4. (*Continued*).

strongly divergent at the mobility edges. We have checked that our direct numerical results essentially agree exactly with the asymptotic analytic theory for the CST potential.

It is clear from the numerical results presented in this section that the asymptotic semiclassical theory developed in the last section is essentially exact for describing the localization properties of the class of slowly varying one-dimensional potentials being studied in this paper. We have numerically verified a number of specific predictions of the theory including the location of the mobility edges at $\pm E_c = \pm|2-\lambda|$ and the asymptotic forms of $D(E)$ and $\gamma(E)$. The theory correctly predicts the critical exponents β and δ for the Lyapunov exponent and the density of states (DOS), respectively, for all the models (the cosine, the square-well, and the more general CST models) studied in this paper. In fact, it is quite surprising that the theory agrees as well as it does with our numerical simulations since some of the simulation results shown here are on rather small ($N \sim 1000$) systems where the local constancy of the potential (which is so crucial for our theoretical arguments) is not very well valid. It is interesting to note that our asymptotic theory which is exact only in the thermodynamic limit works extremely well quite outside the asymptotic regime (or, equivalently, for systems which are rather small in size). We conclude that the predictive ability of the theory is indeed quite good. The reason for this surprising validity of the asymptotic theory for rather small systems is that localization properties of the model depend on $\ln|V_n|$ rather than on V_n and, obviously, $\ln|V_n|$ varies rather weakly.

IV. DISCUSSIONS AND CONCLUSIONS

In this paper we have studied the localization properties of a class of nearest-neighbor one-dimensional tight-binding models where the on-site diagonal potential has a slowly varying period typified by the cosine model $V_n = \lambda \cos(\pi \alpha n^{\nu})$ with $0 < \nu < 1$. We prove, using an asymptotic semiclassical theory which is exact in the thermodynamic limit, that the model has mobility edges at $\pm E_c = \pm|2-\lambda|$ for $\lambda \leq 2$, whereas for $\lambda > 2$ all states are localized. The theory also allows us to derive asymptotically exact expressions for the density of states $D(E)$ and the Lyapunov exponent $\gamma(E)$ for the model as well as their critical exponents β and δ defined by the relations $\gamma(E) \sim |E-E_c|^{\beta}$ and $D(E) \sim |E-E_c|^{-\delta}$. For the cosine (and, the related square-well) model we find β and δ to be 1(0.5) and 0(0.5), respectively. We explicitly verify our theoretical predictions by doing numerical simulation on the tight-binding model using both the direct diagonalization technique and the recursive transfer-matrix technique. An interesting feature of the model is that the variables λ, α, and ν are all irrelevant (in the renormalization group sense) for determining its localization critical properties (the critical point E_c is determined by λ).

Two interesting qualitative features of our results are the existence of mobility edges (and a metal-insulator transition) in a one-dimensional system, and, the singular behavior of the density of states at the mobility edges in this model. Usually, one-dimensional models do not allow for the existence of mobility edges—for example, in the one-dimensional Anderson model random disorder localizes all electron states. To the best of our knowledge

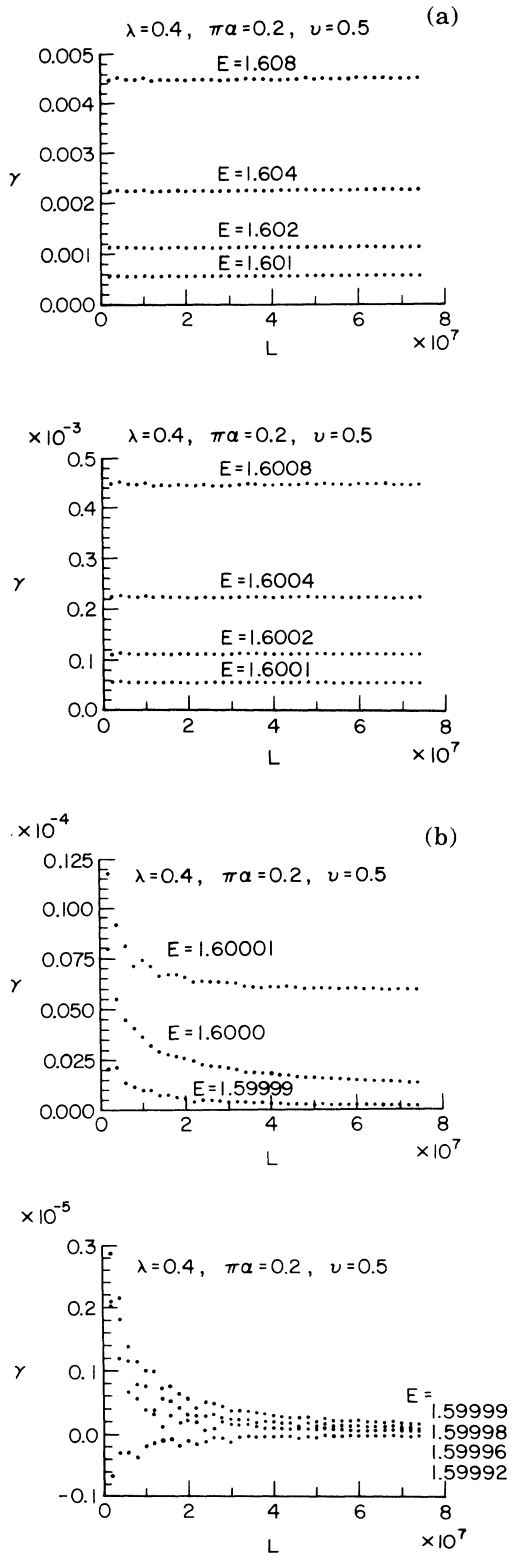

FIG. 5. (a) The singular behavior of the Lyapunov exponent γ when the energy is very close to the mobility edge $E_c = 1.60$ for the cosine potential. γ at various energies are plotted vs the size of the lattice L up to 10^8. The asymptotic value of γ from our numerical calculation agrees completely with the result form WKB calculation. (b) γ at some other energies near the mobility edge $E_c = 1.60$.

this is the *only* known example of a gapless one-dimensional Schrödinger spectrum which has mobility edges separating extended states at the center of the band from localized states at the band edges. The divergent

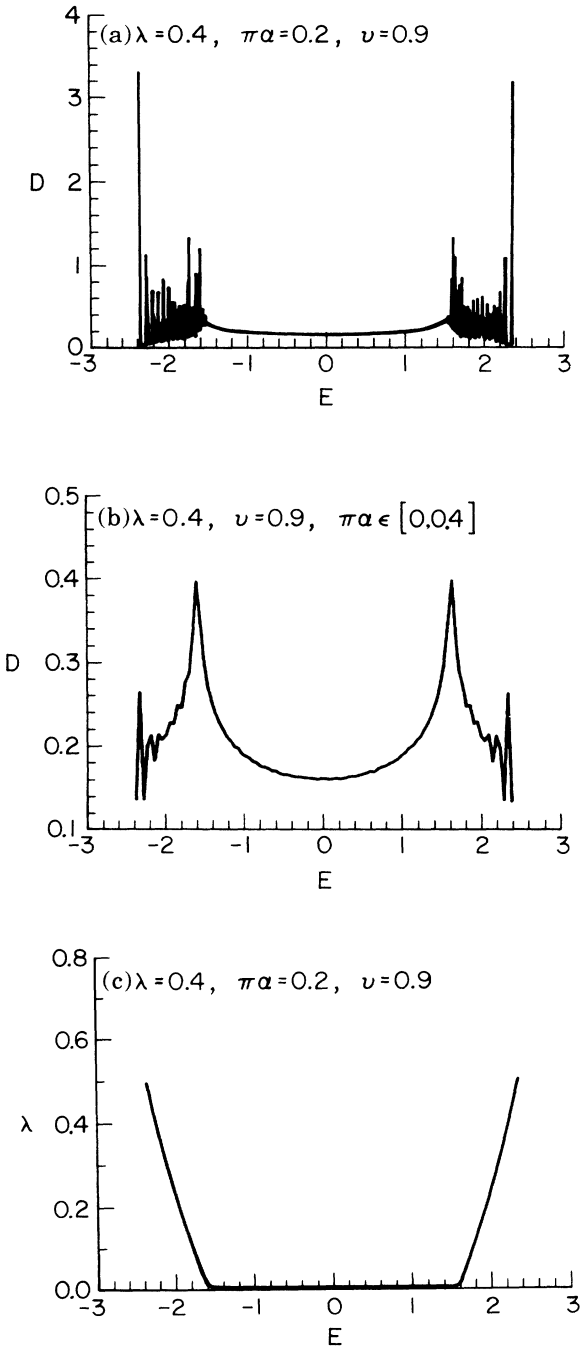

FIG. 6. (a) The DOS for the cosine potential defined in Fig. 3 with the parameter ν changed to 0.9. (b) The average DOS for the cosine potential defined in (a). The singular points of the DOS are at $E_c = 1.60$ or $E_c = -1.60$. (c) The Lyapunov exponent vs energy for the COS potential defined in (a). The mobility edges are at $E_c = 1.60$ or -1.60.

behavior of the density of states, $D(E) \sim |E - E_c|^{-\delta}$ with $\delta > 0$, at the mobility edge is also surprising at first sight because in the three-dimensional random Anderson model $D(E)$ is known to be regular at E_c. As we have discussed in Sec. II, however, the theorem asserting the smooth behavior of $D(E)$ through E_c is inapplicable to our model. Again, to the best of our knowledge, this is the only known example of a metal-insulator transition where the density of states is singular at the transition.

Our semiclassical WKB-type theory asymptotically gives exact results in the thermodynamic limit. In fact, comparison with direct numerical simulation shows that the theory gives quantitatively accurate results even for systems which are only a few thousand sites in size. The theory relies crucially on the very slowly varying nature of the diagonal potential and is valid only in the regime $0 < \nu < 1$. For $\nu \geq 2$ and α irrational, perturbation theory indicates that the system behaves as pseudorandom becoming equivalent to a one-dimensional Anderson model so that all states are localized. In the intermediate regime $1 < \nu < 2$, all states except at $E = 0$ are also localized and the Lyapunov exponent vanishes very slowly at the band center. We emphasize that our nonperturbative theory does not apply for $\nu \geq 1$, whereas the perturbation theory is invalid away from the band center for $\nu < 1$. Perturbation theory, being valid only near the band center and for small λ, does not predict the existence of a mobility edge in this model and gives $\gamma = 0$ everywhere.

The slowly varying nature of the diagonal potential makes the model we are studying *spatially inhomogeneous*, i.e., local regions around different values of n (e.g., very small and very large n's) have very different local potentials. For large n, V_n is locally almost a constant even though the same model potential may be a strongly varying function of n for small n. For any given n, however, the irrelevant parameter α can be varied to change the potential locally. This spatial inhomogeneity of the potential (which exists *only* for $0 < \nu < 1$) distinguishes the mathematical properties of this model from other potentials (e.g., random, incommensurate or the same potential with $\nu > 1$) which have been studied for their interesting

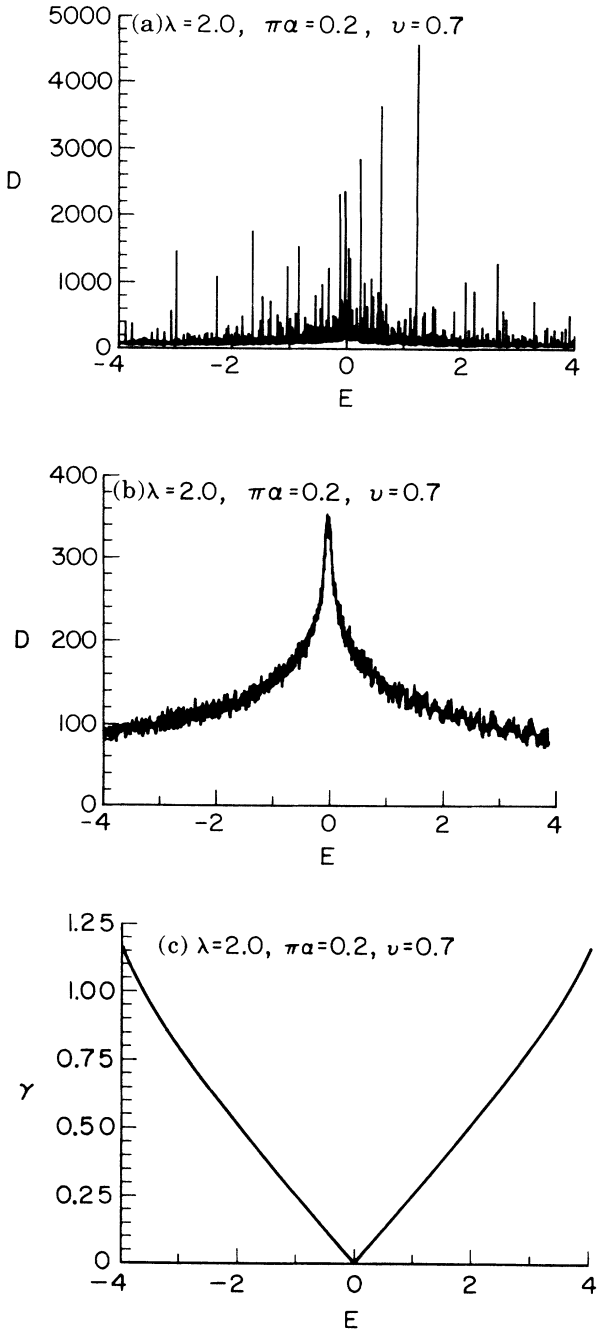

FIG. 7. (a) The DOS for the potential defined in Fig. 1 with the parameter λ changed to 2.0. (b) The average DOS for the cosine potential defined in (a). The DOS is singular only at $E_c = 0.0$. (c) The Lyapunov exponent γ vs energy for the potential defined in (a). One sees that the two mobility edges merge together when $\lambda = 2.0$. The singularity in γ at the mobility edge is linear.

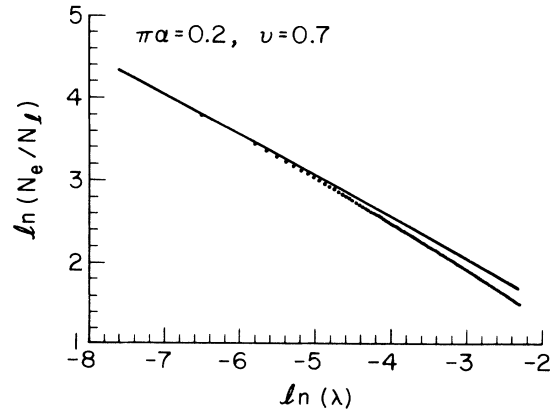

FIG. 8. The ratio of the number of extended states to the number of localized states as a function of the potential strength γ for the cosine potential in a logarithm scale. As can be identified by our numerical calculation, this ratio diverges as $\lambda^{-0.5}$. This result can also be obtained from the WKB theory.

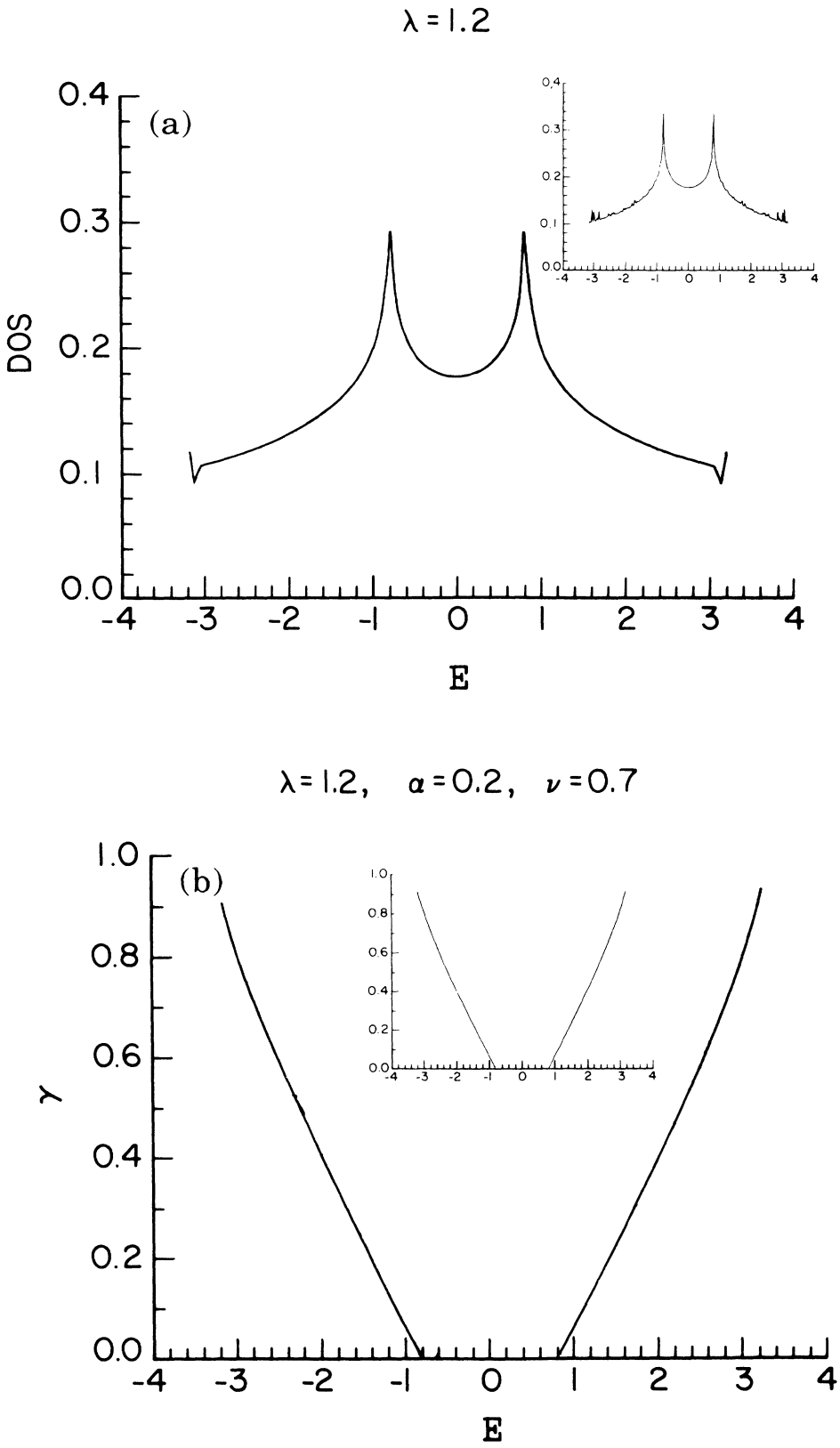

FIG. 9. (a) The DOS for the cosine potential calculated numerically for $\lambda=1.2$. The inset shows the corresponding analytic theoretical result. (b) The Lyapunov exponent versus energy for the cosine model when $\lambda=1.2$. The inset shows the corresponding result from the theoretical analysis.

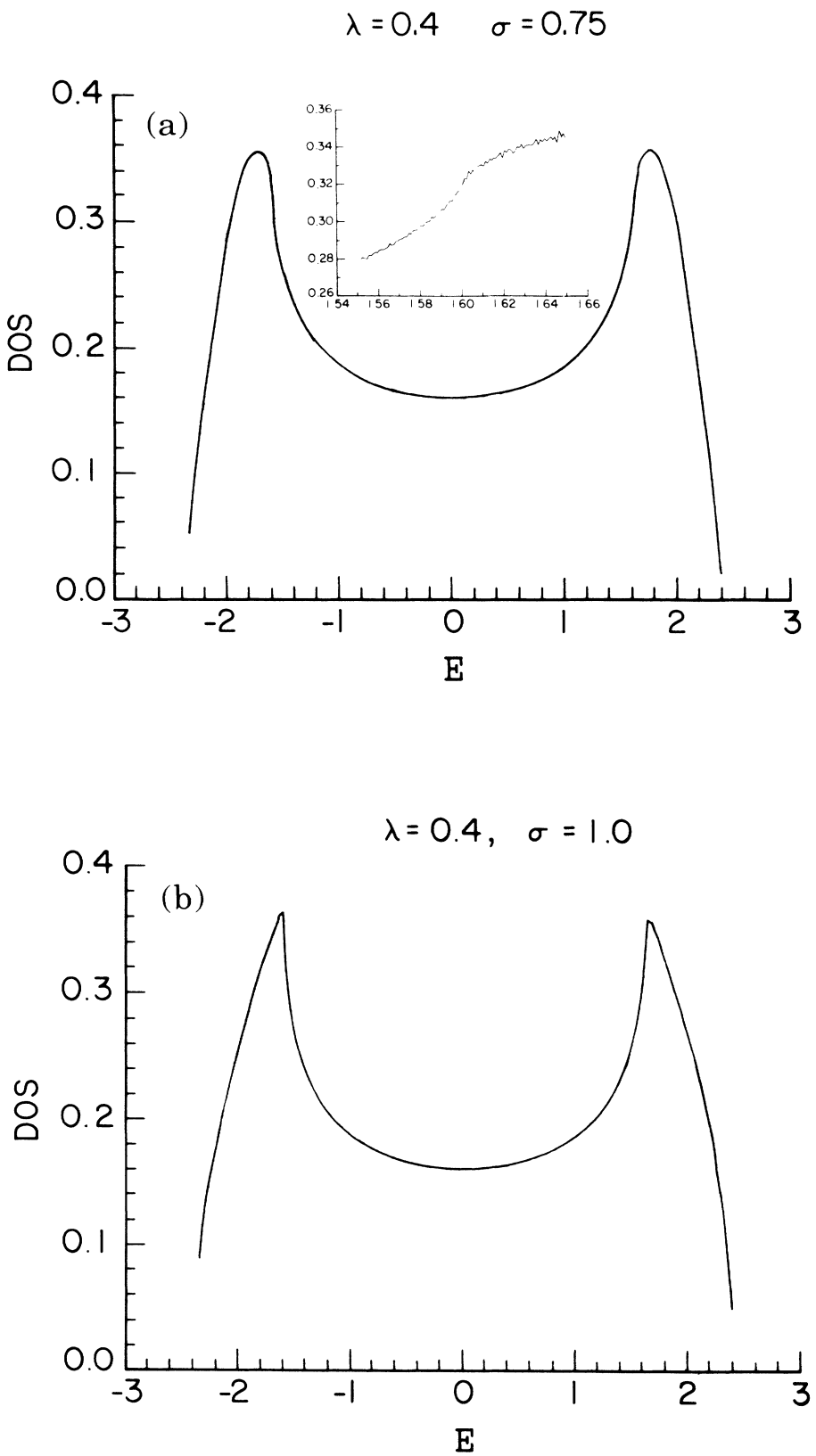

FIG. 10. (a) The DOS for the CST potential calculated numerically for $\lambda=0.4$, $\sigma=0.75$. The inset shows the behavior of the DOS near the mobility edge $E_c=1.6$. (b) The DOS for the CST potential for $\lambda=0.4$, $\sigma=1.0$. (c) The DOS for the CST potential when $\lambda=0.4$, $\sigma=1.5$. The inset shows the behavior of the DOS near the mobility edge $E_c=1.6$. (d) The DOS for the CST potential when $\lambda=0.4$, $\sigma=4.0$. The inset shows the behavior of the DOS near the mobility edge $E_c=1.6$.

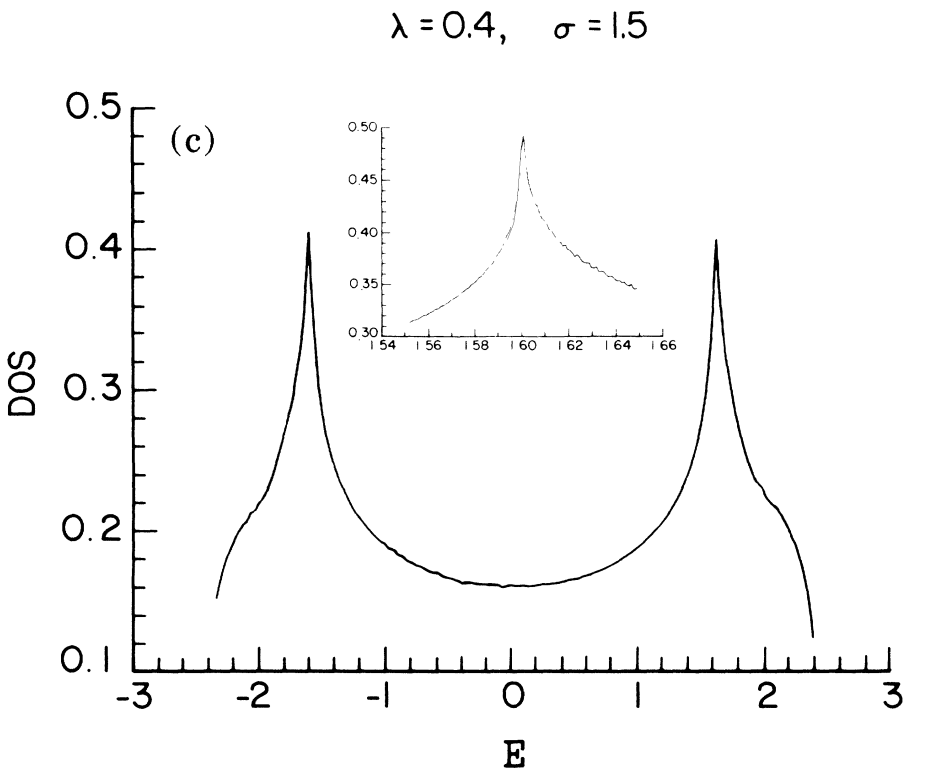

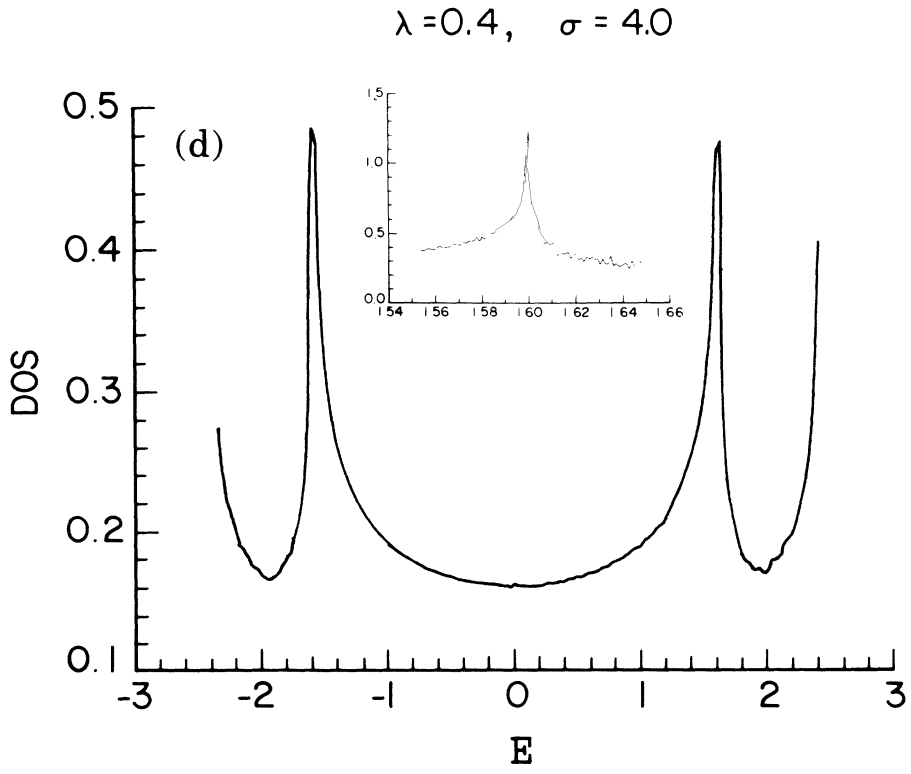

FIG. 10. (*Continued*).

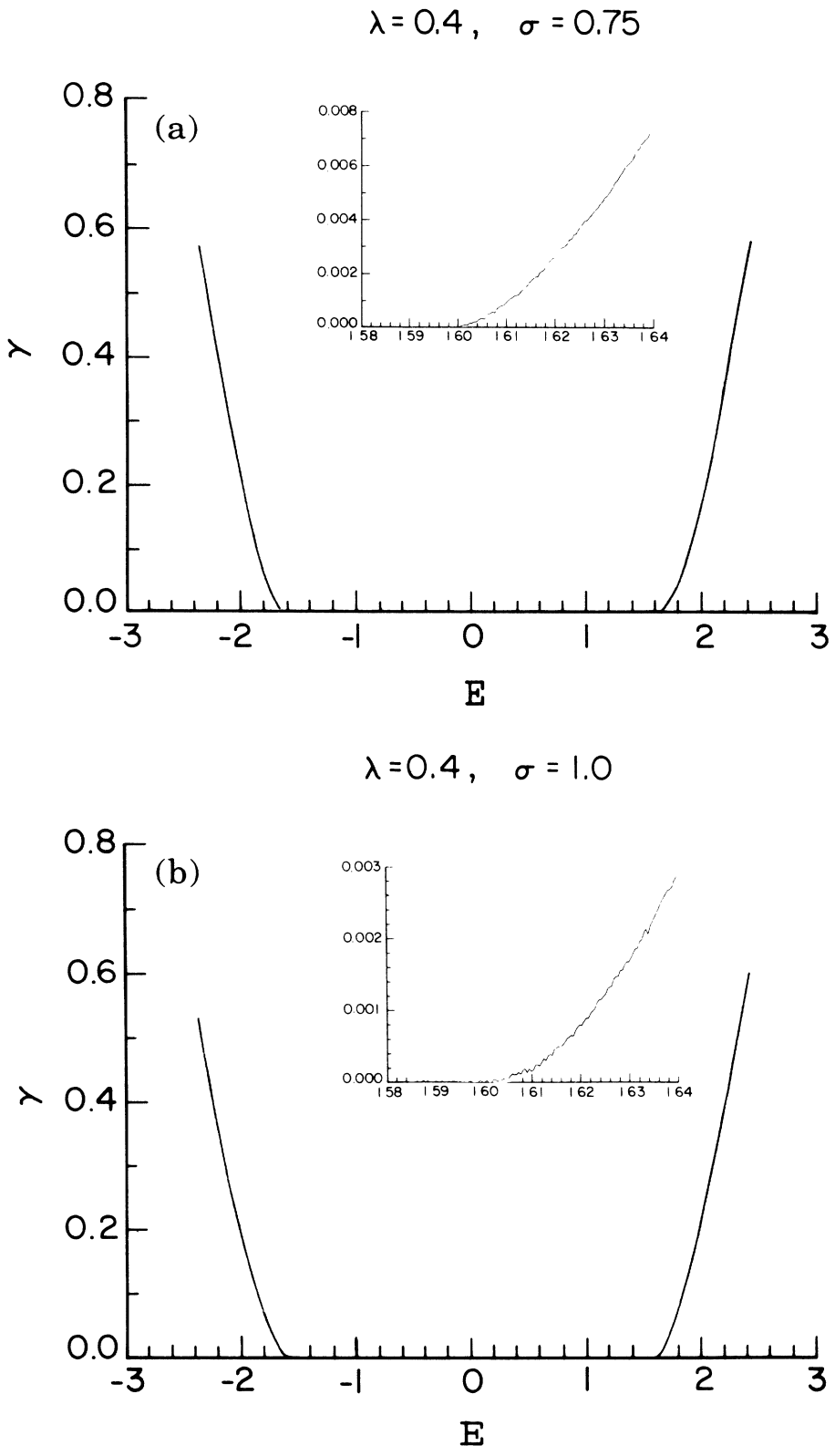

FIG. 11. (a) The Lyapunov exponent vs energy for the CST potential when $\lambda=0.4$, $\sigma=0.75$. The inset shows the behavior of the Lyapunov exponent near the mobility edge $E_c=1.6$. (b) The Lyapunov exponent vs energy for the CST potential when $\lambda=0.4$, $\sigma=1.0$. The inset shows the behavior of the Lyapunov exponent near the mobility edge $E_c=1.6$. (c) The Lyapunov exponent γ vs energy for the CST potential when $\lambda=0.4$, $\sigma=1.5$. The inset shows the behavior of γ near $E_c=1.6$. (d) The Lyapunov exponent γ vs energy for the CST potential when $\lambda=0.4$, $\sigma=4.0$. The inset shows the behavior of γ near $E_c=1.6$.

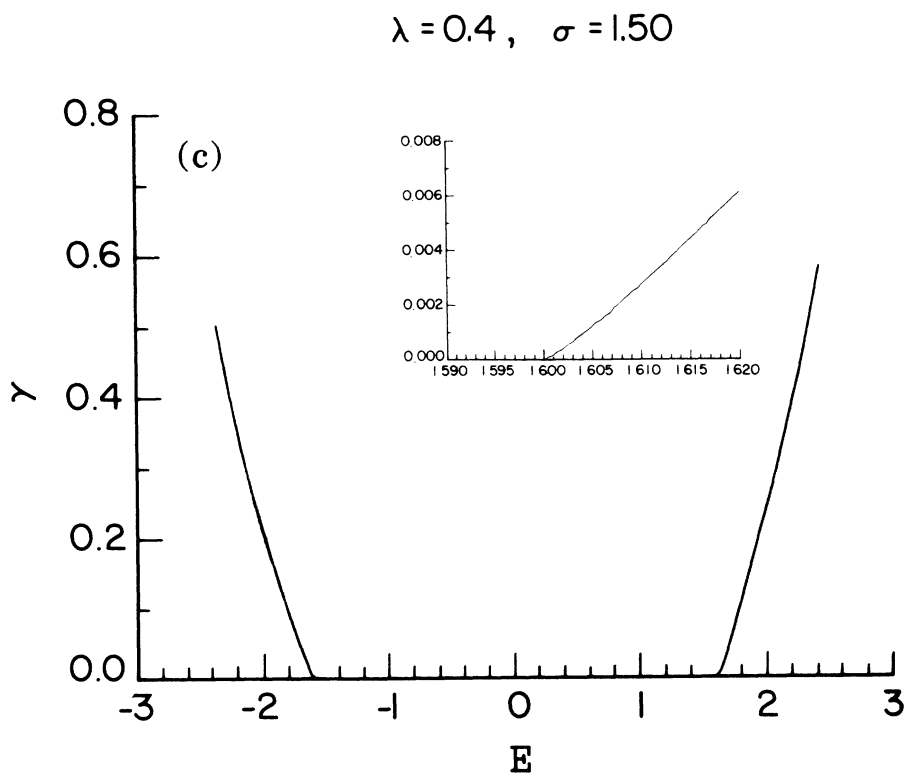

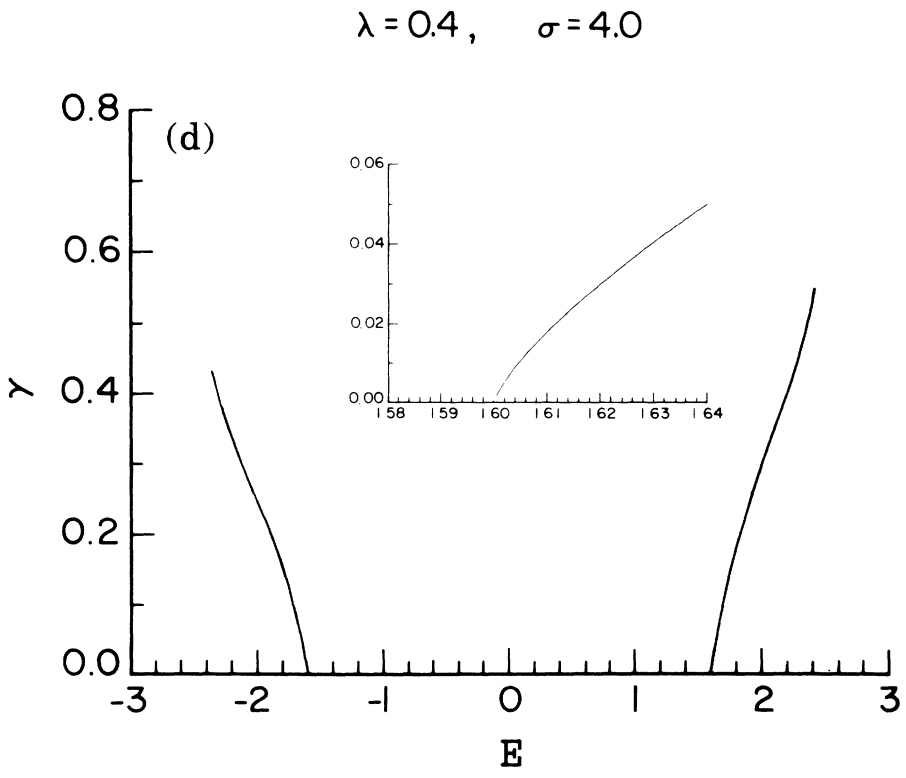

FIG. 11. (*Continued*).

localization properties. Not much is rigorously known about the mathematical properties of such spatial inhomogeneous systems. We hope that our work will generate some interest in that direction.

There are a number of open questions which we have not discussed so far. These include possible experimental relevance of our results, transport properties of the model, effects of longer-range hopping on the theory (the model has so far been strictly a nearest-neighbor one), and possible connection of this model to other types of localization problems. We have calculated some preliminary transport properties of the model using the Landauer formula and a metal-insulator transition shows up at $E=E_c$.

We believe that potentially the best method of observing the metal-insulator transition discussed in this paper is to do transport experiments on artificially structured semiconductor superlattices[10] where a background potential can be introduced by suitable computer-controlled doping using the molecular-beam-epitaxy (MBE) technique. Transport experiments[20] along the superlattice growth direction are fairly standard now and MBE growth technique is mature enough to allow for precisely computer-controlled potential profile. One should be able to observe the metal-insulator transition predicted in this paper in such artificially structured semiconductor superlattices as the Fermi energy moves through the mobility edge. A potentially very significant problem in any experimental study of the theory developed here is the role that random disorder, invariably present in any real system, will play in such experiments. Since in one dimension any disorder leads to localization, the question of whether the metal-insulator transition predicted here can ever be observed experimentally is an important one. We believe that for a very weak disorder (compared with the strength λ of the slowly varying potential), the disorder-induced localization length would be very large and the metal-insulator transition predicted in this work should be experimentally observable. Clearly, the interplay between a (weak) random potential and the slowly varying potential studied here is an interesting problem which deserves further attention.

Transport properties of the model also need to be theoretically investigated. At this stage, we can only say that the system would change from being a conductor to an insulator as the Fermi level is pushed from below E_c to above it. Particularly interesting is the question of how the conductivity scales with $|E-E_c|$ around the mobility edge. Since our theory gives asymptotically exact expressions for the Lyapunov exponent and the density of states, it seems that a theory for calculating the conductivity of our model is, in principle, be worked out. That is, however, beyond the scope of this work where we are concentrating on the one-electron properties of the model.

We have, in a very limited way, numerically investigated the effect of longer-range hopping on the localization transition in the cosine model by including a next-nearest-neighbor hopping term in the tight-binding Eq. (1) which now becomes

$$t(u_{n-2}+u_{n+2})+(u_{n-1}+u_{n+1})+V_n u_n=Eu_n \ , \tag{44}$$

with t as the strength of the next-nearest-neighbor coupling term. We have used the direct diagonalization technique to obtain the eigenfunctions and the eigenenergies of Eq. (44). We have also extended our semiclassical arguments to include the next-nearest-neighbor hopping. For weak next-nearest-neighbor hopping, specifically for $t \leq \frac{1}{4}$, we find that the only effect of the next-nearest-neighbor term is to shift the critical region by modifying the locations of the mobility edges which are now at $E=E_c^{(\pm)}$, where

$$E_c^{(+)}=(2-\lambda)+2t \ , \tag{45a}$$

$$E_c^{(-)}=-(2-\lambda)+2t \ . \tag{45b}$$

Thus, the new mobility edges are at

$$E_c^{(\pm)}=\pm E_c+2t \ , \tag{46}$$

where $\pm E_c$ are the original mobility edges for the nearest-neighbor model.

For higher values of t, the model seems to have very rich and complex localization properties with *more than two* mobility edges. We have identified three or four mobility edges depending on the situation. To clarify the situation requires substantial work which is beyond the scope of the present work. We note that, in general, not much is known about the effect of long-range hopping on the localization transition even in the extensively studied random Anderson model.

Finally, the relationship of the metal-insulator transition in the slowly varying potential studied here to the usual metal-insulator transition in the random Anderson case is not very clear to us. Electron localization is a quantum interference phenomenon and, normally, WKB-type local semiclassical argument is of no use in studying the localization problem. In this problem, however, the spatial inhomogeneity associated with the extreme slow variation of the diagonal potential in the thermodynamic limit makes the asymptotic semiclassical analysis an exact one. Diagrammatic scattering theoretic techniques[21] and field-theoretic methods[22] have been helpful in studying the localization transition in randomly disordered systems. Whether such a field theory exists for the localization transition studied in this paper remains an intriguing open question.

We conclude by pointing out an aspect of our theory which has been emphasized earlier in this paper. Our assertion has been that *all* slowly varying asymptotically locally constant potentials lead to the same mobility edges $\pm E_c=\pm|2-\lambda|$, determined only by the maximum strength of the potential. Another theoretical claim is that the critical exponents of the theory depend *only* on the local curvature of the potential around its minimum in the thermodynamic limit and parameters such as λ,α,ν are all irrelevant in the renormalization group sense. We have "verified" these theoretical assertions by numerically studying three model potentials (i.e., the CST, the cosine, and the square-well model). It is interesting to conclude this paper by pointing out that a counter-example will severely question the validity of our whole theoretical approach.

ACKNOWLEDGMENTS

One of the authors (S.D.S.) thanks Professor S. Fishman and Professor R. E. Prange for a number of stimulating discussions. The authors thank Professor Fishman for a critical reading of the manuscript as well. This work has been supported by the U.S. National Science Foundation (NSF) and the U.S. Office of Naval Research (ONR), U.S. Department of Defense. The authors are grateful to the University of Maryland Computing Center for providing the computer time needed for this work.

APPENDIX A

The purpose of this appendix is to discuss, for the sake of completeness, the perturbation calculation by Griniasty and Fishman[11,12] for the cosine model, namely,

$$u_{n+1}+u_{n-1}+\lambda\cos(\pi\alpha n^{\nu})u_{n+1}=Eu_n \ . \tag{A1}$$

In the following, the on-site potential $V_n=\lambda\cos(\pi\alpha n^{\nu})$ will be taken as a perturbation.

Obviously, the Green's function for Eq. (A1) when $\lambda=0$ is

$$G^0=\frac{1}{2\pi}\int_0^{2\pi}d\theta\frac{1}{E+i\eta-2\cos\theta} \ , \tag{A2}$$

where $|\theta\rangle$ is a plane-wave eigenstate, i.e., $\langle n|\theta\rangle=e^{in\theta}/N^{1/2}$ and $N\to\infty$ being the total length of the lattice.

From Eq. (A2), we have the matrix element[15,17] of the G^0 as

$$\langle n|G^0|m\rangle=e^{-i\theta|m-n|}/(2i\sin\theta) \ , \tag{A3}$$

where θ is given by

$$E=2\cos\theta \ . \tag{A4}$$

Using Dyson's equation, we have the full Green's function as

$$G=G^0+G^0VG \ , \tag{A5}$$

where $\langle n|V|m\rangle=\lambda\cos(\pi\alpha n^{\nu})\delta_{n,m}$. To the lowest order of λ, we have

$$G=G^0+G^0VG^0 \ . \tag{A6}$$

Now, our goal is to use a result by Thouless[17] to find the Lyapunov exponent $\gamma(E)$ by

$$\gamma(E)=\lim_{n\to\infty}\left[\ln\left|\frac{G_{NN}(E)}{G_{1N}(E)}\right|\Big/N\right] \ . \tag{A7}$$

Now, our next step is to find the matrix elements G_{NN} and G_{1N}. Combining (A3) and (A6), we get

$$\langle N|G|N\rangle=\langle N|G^0|N\rangle+\sum_n|\langle N|G^0|n\rangle|^2V_n \tag{A8}$$

$$=\frac{1}{2i\sin\theta}-\left[1+\frac{1}{2i\sin\theta}\sum_n V_n e^{-2i\theta(N-n)}\right] \ , \tag{A9}$$

$$\langle 1|G|N\rangle=\langle 1|G^0|N\rangle+\sum_n\langle 1|G^0|n\rangle\langle n|G^0|N\rangle V_n \tag{A10}$$

$$=\frac{e^{i(N-1)}}{2i\sin\theta}\left[1+\frac{1}{2i\sin\theta}\sum_n V_n\right] \ . \tag{A11}$$

Now, from (A7), (A9), and (A11)

$$\gamma(E)=\lim_{n\to\infty}\left[\frac{1}{N}\ln\left|\frac{1+\frac{1}{2i\sin\theta}\sum_n V_n e^{2in\theta}}{1+\frac{1}{2i\sin\theta}\sum_n V_n}\right|\right] \ . \tag{A12}$$

From $V_n=\lambda\cos(\pi\alpha n^{\nu})$, $\nu>0$, we have, by virtue of ergodicity,

$$\lim_{n\to\infty}\left[\frac{1}{N}\sum_n V_n e^{-2in\theta}\right]=0 \tag{A13}$$

and

$$\lim_{n\to\infty}\left[\frac{1}{N}\sum_n V_n\right]=0 \ . \tag{A14}$$

Using (A14), (A15), and (A16), we obtain

$$\gamma(E)=\lim_{n\to\infty}\left[\frac{1}{N}\ln\left[1+\frac{1}{4\sin^2\theta}\left|\sum_n V_n e^{2in\theta}\right|\right]\right] \ . \tag{A15}$$

For λ small enough and θ far away from 0 and π, (A15) gives

$$\gamma(E)=\lim_{N\to\infty}\left[\frac{\lambda^2}{8N\sin^2\theta}|S_N|^2\right] \ , \tag{A16}$$

where $S_N=(S_N^+ +S_N^-)$ with

$$S_N^{\pm}=\sum_{n=1}^{N}e^{i(2n\theta\pm\pi\alpha n^{\nu})} \ . \tag{A17}$$

Now, let us find the asymptotic behavior of $|S_N|^2/N$ as $N\to\infty$.

First of all, from a result by Hardy and Littlewood,[23] for the case when $\nu=2$ and α irrational

$$S_N\sim N^{1/2} \ \text{ as } N\to\infty \ . \tag{A18}$$

In fact, $\cos(\pi\alpha n^{\nu})$ is random-walk-like when $\nu\geq 2$ with α being some generic irrational numbers. Then

$$|S_N|^2=N/2+o(N) \ . \tag{A19}$$

Therefore, when $\nu\geq 2$, α irrational

$$\gamma(E)=\frac{\lambda^2}{16\sin^2\theta} \ . \tag{A20}$$

Secondly, when $1<\nu<2$, we can rewrite (A17) as the following by the Poisson formula:

$$S_N^+=\sum_m\int_0^N dn\,\exp[i(\pi\alpha n^{\nu}+2n\theta-2\pi mn)] \ . \tag{A21}$$

Using stationary phase method, the above equation becomes

$$S_N^+ = A \sum_n m^{\beta/2} \exp(i\pi\alpha' m^{\nu'}) , \tag{A22}$$

where $\nu'=\nu/(\nu-1)$, $\beta=(2-\nu)/(\nu-1)$, $B=2/(\alpha\nu)$, $\alpha'=\alpha B^{\nu'}-2B^{1/(\nu-1)}$, and $M=N^{\nu-1}/B$. The constant $A=B^{\beta/2}[\alpha\nu(\nu-1)]^{1/2}(1+i)$.

When $1<\nu<2$, we have $\nu'>2$; then, to the lowest order of $1/N$

$$|S_N|^2=|S_N^+ + S_N^-|^2/4=|S_N^+|/2=\tfrac{1}{2}|A|^2 \sum_n m^{\beta/2} \tag{A23}$$

$$=|A|^2 M^{\beta+1}/2=N/2 . \tag{A24}$$

Hence, for $1<\nu<2$

$$\gamma(E)=\frac{\lambda^2}{16\sin^2\theta} .$$

From the above derivation, when $0<\nu<1$, (A22) becomes

$$S_N^+ = AO\left[\sum_n m^{\beta/2}\right] \tag{A25}$$

which is convergent. Then $\gamma(E)=0$. As a conclusion

$$\gamma(E)=\begin{cases} \dfrac{\lambda^2}{16\sin^2\theta} & \text{for } \nu>1 , \\ 0 & \text{for } 0<\nu\le 1 . \end{cases}$$

We emphasize that the perturbation calculation is not valid away from the band center for $\nu<1$.

APPENDIX B

In this appendix we discuss the singular behavior of the DOS near the mobility edge E_c and band edge E_b for the cosine and square-well models. From Eq. (31), we have

$$D(E)=\frac{1}{2\pi}\int_{-T/2}^{T/2}\frac{1}{T}dx \ \mathrm{Re}\left[\frac{1}{\left[1-\dfrac{(E-f)^2}{4}\right]^{1/2}}\right] . \tag{B1}$$

For simplicity, we change the scale and origin of x such that Eq. (B1) becomes

$$D(E)=\frac{1}{2\pi}\int_0^1 dx \ \mathrm{Re}\left[\frac{1}{\left[1-\dfrac{(E-f)^2}{4}\right]^{1/2}}\right] \tag{B2}$$

with $f(0)=-\lambda$, $f(1)=\lambda$ ($\lambda>0$).

Now, we begin to discuss the behavior of the DOS near $E_c=2-\lambda$. For this purpose, we write

$$f(x)=-\lambda+g(x) \tag{B3}$$

with $g(0)=0, g(1)=2\lambda$.

First, we look at the case when $E=E_c-\Delta$, $\Delta>0$. From (B2), we can get

$$D(E)=\frac{1}{2\pi}\int_0^1 dx \ \mathrm{Re}\left[\frac{1}{(1-\{1-\frac{1}{2}[\Delta+g(x)]\}^2)^{1/2}}\right] . \tag{B4}$$

Obviously, when $0<\lambda<2$

$$|1-\tfrac{1}{2}[\Delta+g(x)]|<1 \tag{B5}$$

and then (B4) becomes

$$D(E)=\frac{1}{2\pi}\int_0^1 dx \frac{1}{(1-\{1-\frac{1}{2}[\Delta+g(x)]\}^2)^{1/2}} . \tag{B6}$$

To see the behavior of $D(E)$ clearly, let us write (B6) as

$$D(E)=\frac{1}{2\pi}\left[\int_{x_0}^1 dx \frac{1}{(1-\{1-\frac{1}{2}[\Delta+g(x)]\}^2)^{1/2}} + \int_0^{x_0} dx \frac{1}{(1-\{1-\frac{1}{2}[\Delta+g(x)]\}^2)^{1/2}}\right] \tag{B7}$$

with $x_0>0$.

Now, the first term in (B7) will contribute a regular part to $D(E)$, i.e.,

$$\frac{1}{2\pi}\int_{x_0}^1 dx \frac{1}{(1-\{1-\frac{1}{2}[\Delta+g(x)]\}^2)}=D_0+D_1\Delta+o(\Delta) \tag{B8}$$

as $\Delta\to 0^+$.

Let us now analyze the second term in (B7). For this purpose, we assume that $g(x)=g_0x^\sigma+o(x^\sigma)$ as $x\to 0^+$. We choose x_0 such that $g(x)=g_0x^\sigma+o(x^\sigma)=g_0x^\sigma$ will be a good approximation of $g(x)$ when $\phi<x<x_0$, then, the second term in Eq. (B7) becomes

$$D_{\mathrm{II}}=\frac{1}{2\pi}\int_0^{x_0} dx \frac{1}{\{1-[1-\frac{1}{2}(\Delta+g_0x^\sigma)]^2\}^{1/2}} \tag{B9}$$

$$=\frac{1}{2\pi}\int_0^{x_0} dx \frac{1}{(\Delta+g_0x^\sigma)^{1/2}}\frac{1}{[1-\frac{1}{4}(\Delta+g_0x^\sigma)]^{1/2}} \tag{B10}$$

$$\sim\frac{1}{2\pi}\int_0^{x_0} dx \frac{1}{(\Delta+g_0x^\sigma)^{1/2}} , \tag{B11}$$

where the factor $1/[1-\frac{1}{4}(\Delta+g_0x^\sigma)]^{1/2}$ has been dropped because it only contributes a regular factor $1+O(\Delta)$ as $\Delta\to 0^+$ when $0<\lambda<2$.

Now, we can write (B11) into

$$D_{\mathrm{II}}\sim\frac{1}{2\pi}g_0^{-1/\sigma}\Delta^{1/\sigma-1/2}\int_0^{x_0 g_0^{1/\sigma}/\Delta^{1/\sigma}} dy\frac{1}{(1+y^\sigma)^{1/2}} , \tag{B12}$$

where $y=x(g_0/\Delta)^{1/\sigma}$.

We note the following: (1) when $\sigma>2$, the integral

$$\int_0^{x_0 g_0^{1/\sigma}/\Delta^{1/\sigma}} dy\frac{1}{(1+y^\sigma)^{1/2}}=\int_0^{+\infty} dy\frac{1}{(1+y^\sigma)^{1/2}} \tag{B13}$$

converges as $\Delta \to +0$.

Then

$$D_{\rm II} \sim \frac{1}{2\pi} g_0^{-1/\sigma} \Delta^{1/\sigma - 1/2} \int_0^{+\infty} dy \frac{1}{(1+y^\sigma)^{1/2}}$$

contributes a singular part to $D(E)$.

Obviously, the exponent for the DOS is $\delta = \frac{1}{2} - 1/\sigma$; (2) when $\sigma = 2$, the integral $\int_0^{x_0 g^{1/\sigma}/\Delta^{1/\sigma}} dy\, 1/(1+y^\sigma)^{1/2}$ diverges; its asymptotic behavior can be found to be

$$\int^{x_0 g^{1/\sigma}/\Delta^{1/\sigma}} dy \frac{1}{y^{\sigma/2}} = \ln\left[\frac{x_0 g_0^{1/\sigma}}{\Delta^{1/\sigma}}\right] + o(\ln\Delta) \quad \text{(B14)}$$

as $\Delta \to 0^+$ when $\sigma = 2$.

Then

$$D_{\rm II} \sim \frac{1}{2\pi} g_o^{-1/\sigma} \frac{1}{\sigma} \ln(1/\Delta) + o(\ln\Delta) \; . \quad \text{(B15)}$$

Obviously, $D_{\rm II}$ is again singular. Therefore $D(E)$ has an exponent $\delta = 0$ when $\sigma = 2$.

Similarly, as $E \to E_c + 0$, we obtain the same results for δ. Summing up the above discussion

$$x = \begin{cases} \delta = \frac{1}{2} - 1/\sigma & \text{if } \sigma > 2 \; , \\ \delta = 0(\log) & \text{if } \sigma = 2 \; , \\ \delta = -1 & \text{if } 0 < \sigma < 2 \; . \end{cases}$$

Note that the critical exponent for the Lyapunov exponent near E_c is $\beta = \frac{1}{2} + 1/\sigma$, then we see that $\beta + \delta = 1$ holds only when $\sigma \geq 2$.

Next, for the singular behavior of $D(E)$ near the band edges $E_B = \pm(2+\lambda)$. Let us scale x and change its origin such that (B1) can be written into

$$D(E) = \frac{1}{2\pi} \int_0^1 dx \, \mathrm{Re} \frac{1}{\left[1 - \frac{(E-f)^2}{2}\right]^{1/2}} \; , \quad \text{(B16)}$$

where $f(0) = \lambda$, $f(1) = -\lambda$.

For the purpose of our discussion, let us write

$$f(x) = \lambda - g(x) \quad \text{with } g(0) = 0, \quad g(1) = 2\lambda \; .$$

Then, (B16) becomes

$$D(E) = \frac{1}{2\pi} \int_0^1 dx \, \mathrm{Re} \left[\frac{1}{(1 - \{1 - \frac{1}{2}[\Delta + g(x)]\}^2)^{1/2}} \right] \quad \text{(B17)}$$

if $E = E_B - \Delta = 2 + \lambda - \Delta$ and $\Delta \to 0^+$. Now, we assume x_c to be such that $\Delta = g(x_c)$; then (B17) becomes

$$D(E) = \frac{1}{2\pi} \int_0^{x_c} dx \frac{1}{(1 - \{1 - \frac{1}{2}[\Delta + g(x)]\}^2)^{1/2}} \quad \text{(B18)}$$

as $\Delta \to 0^+$, $x_c \to 0^+$. Let $g(x) = g_0 x^\sigma + o(x^\sigma)$:

$$D(E) \sim \frac{1}{2\pi} g_0^{-1/\sigma} \Delta^{1/\sigma - 1/2} \int_0^1 dy \frac{1}{(1+y^\sigma)^{1/2}} \; , \quad \text{(B19)}$$

where $y = (g_0/\Delta)^{1/\sigma} x$.

Obviously, (1) when $\sigma > 2$, $D(E)$ diverges as $E \to E_B - 0$, the exponent is $\delta = \frac{1}{2} - 1/\sigma$; (2) When $\sigma = 2$, $D(E)$ converges to a constant:

$$\begin{aligned} D(E) &= \frac{1}{2\pi} g_0^{-1/\sigma} \int_0^1 dy \frac{1}{(1+y^\sigma)^{1/2}} \\ &= \frac{1}{2\pi} g_0^{-1/\sigma} \int_0^1 dy \frac{1}{(1+y^\sigma)^{1/2}} \\ &= \frac{1}{4\sqrt{g_0}} \quad \text{as } E \to E_B - 0 \; ; \end{aligned}$$

(3) When $0 < \sigma < 2$, $D(E)$ vanishes with an exponent $\delta = \frac{1}{2} - 1/\sigma$ as

$$D(E) \sim |E - E_B|^{1/\sigma - 1/2} = |E - E_B|^{-\delta} \; .$$

[1] P. W. Anderson, Phys. Rev. **109**, 1492 (1958).

[2] D. J. Thouless, Phys. Rep. **13**, 95 (1974); P. A. Lee and T. V. Ramakrishnan, Rev. Mod. Phys. **57**, 287 (1985), and references therein.

[3] S. Aubry and G. Andre, Ann. Isr. Phys. Soc. **3**, 133 (1979).

[4] For reviews on the incommensurate potential, see J. B. Sokoloff, Phys. Rep. **126**, 189 (1985); B. Simon, Adv. Appl. Math. **3**, 463 (1982).

[5] See, for example, N. W. Ashcroft and D. Mermin, *Solid State Physics* (Holt, Rinehart and Winston, New York, 1976).

[6] K. Ishii, Prog. Theor. Phys. Suppl. **53**, 77 (1973).

[7] D. R. Grempel, S. Fishman, and R. E. Prange, Phys. Rev. Lett. **49**, 833 (1982).

[8] J. Belissard, D. Bessis, and P. Moussa, Phys. Rev. Lett. **49**, 701 (1982).

[9] M. Kohmoto, L. P. Kadanoff, and C. Tang, Phys. Rev. Lett. **50**, 1870 (1983); S. Ostlund *et al.*, *ibid.* **50**, 1873 (1983).

[10] S. Das Sarma, A. Kobayashi, and R. E. Prange, Phys. Rev. Lett. **56**, 1280 (1986); Phys. Rev. B **34**, 5309 (1986).

[11] J. Adler, M. Griniasty, and S. Fishman (unpublished).

[12] M. Griniasty and S. Fishman, Phys. Rev. Lett. **60**, 1334 (1988).

[13] A. Crisanti (unpublished).

[14] S. Das Sarma, S. He, and X. C. Xie, Phys. Rev. Lett. **61**, 2144 (1988).

[15] D. J. Thouless, Phys. Rev. Lett. **61**, 2141 (1988).

[16] M. V. Berry and J. Goldberg, Nonlinearity **1**, 1 (1987).

[17] D. J. Thouless, J. Phys. C **5**, 77 (1972); **6**, L49 (1973); see also V. Osceledec, Trans. Moscow. Math. Soc. **19**, 197 (1968); J. L. Pichard, J. Phys. C **19**, 1519 (1986).

[18] See, for example, L. D. Landau and I. Lifshitz, *Quantum Mechanics* (Pergamon, Oxford, 1965).

[19] J. T. Edwards and D. J. Thouless, J. Phys. C **4**, 453 (1971).

[20] S. R. Yang and S. Das Sarma, Phys. Rev. B **37**, 10090 (1988), references therein.

[21] D. Volhardt and P. Wöfle, Phys. Rev. B **22**, 4666 (1980).

[22] F. Wegner, Z. Phys. **35**, 207 (1979).

[23] G. H. Hardy and J. E. Littlewood, Acta Math. **37**, 193 (1914).